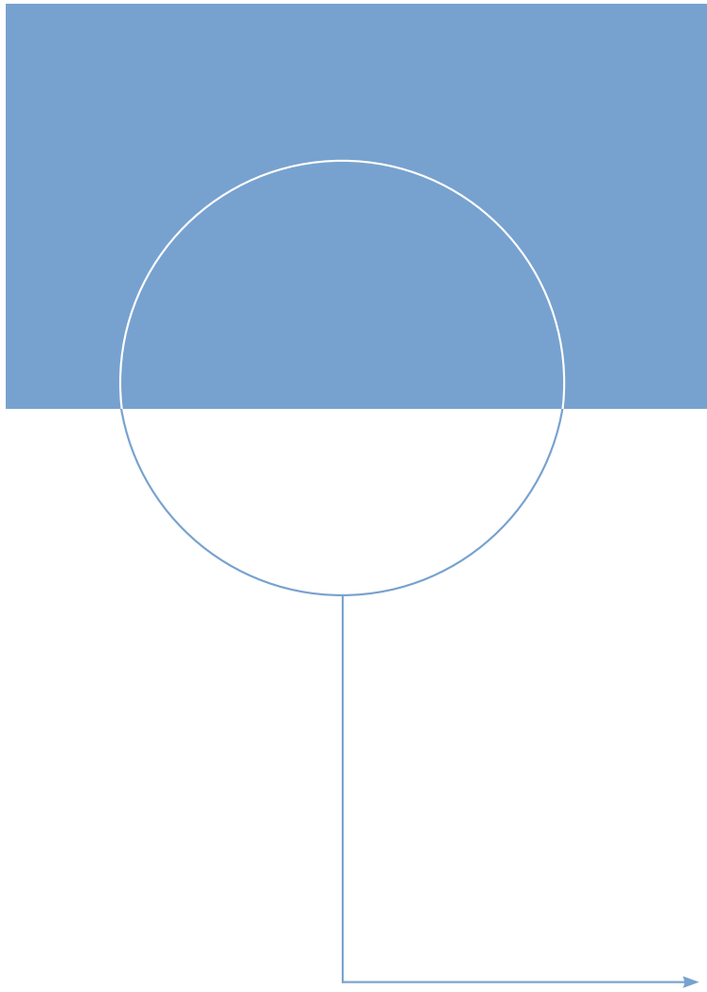

Master's thesis

2019

Ina Bjørkum Arneson

NTNU
Norwegian University of
Science and Technology
Faculty of Engineering
Department of Marine Technology

Ina Bjørkum Arneson

Towards Autonomous Ships

Sea State Estimation and Risk-Based Decision Making

June 2019

NTNU
Norwegian University of
Science and Technology

NTNU
Norwegian University of
Science and Technology

NTNU

Norwegian University of
Science and Technology

Towards Autonomous Ships

Sea State Estimation and Risk-Based Decision Making

Ina Bjørkum Arneson

Marine Technology
Submission date: June 2019
Supervisor: Asgeir J. Sørensen and Ingrid B. Utne
Co-supervisor: Astrid H. Brodtkorb and Børge Rokseth

Norwegian University of Science and Technology
Department of Marine Technology

NTNU Trondheim
Norwegian University of Science and Technology
Department of Marine Technology

MASTER THESIS IN MARINE CYBERNETICS

SPRING 2019

FOR

STUD. TECHN. INA BJØRKUM ARNESON

Towards Autonomous Ships

Work description (short description)
Situation awareness is a research area of great importance in the development of autonomous ships. An autonomous ship must be at least as safe as a humanly operated ship and is therefore dependent on extensive knowledge of its surroundings to be able to make safe and correct decisions.

The aim of this thesis is to develop a sea state estimation algorithm based on machine learning methods, as a continuance of previous work, as well as developing an online decision model. The thesis will be composed of a resume and two scientific papers. The first paper will be on sea state estimation for a vessel in dynamic positioning (DP). The second paper will propose an online decision model for collision avoidance for a DP vessel.

Scope of work

Resume:
- Background and literature study on autonomy and situation awareness
- Background information and literature study on sea state estimation
- Additional results not presented in the appended papers
- Conclusions and further work

Paper A:
- Demonstration of a sea state estimation algorithm for estimating wave direction, significant wave height and peak wave period for a vessel in DP
- Presentation of sea state estimation results

Paper B:
- Construction of a Bayesian Belief Network (BBN) for calculating collision risk
- Integration of BBN in an online decision model in a DP setting
- Demonstration of simulation and model experiment results testing the model on synthetic scenarios

NTNU Trondheim
Norwegian University of Science and Technology
Department of Marine Technology

The report shall be written in English and edited as a collection of articles with a resume in front, in a report format. It is supposed that Department of Marine Technology, NTNU, can use the results freely in its research work, unless otherwise agreed upon, by referring to the student's work.

The thesis should be submitted within 11th of June.

Advisors: Astrid H. Brodtkorb and Børge Rokseth

Professor Asgeir J. Sørensen
Professor Ingrid B. Utne
Supervisor

Abstract

The overall topic of this thesis is situation awareness in autonomous systems. The thesis is divided into two parts, where the first is related to estimating the sea state of a dynamically positioned (DP) vessel, and the second is about decision-making related to collision risk for a DP vessel. These topics are highly relevant for research on autonomous ships, as the sea state is a crucial input to an autonomous decision system.

A sea state estimation algorithm independent of the vessel transfer function has been developed for a vessel in DP. The algorithm uses Quadratic Discriminant Analysis for estimating the absolute wave direction, and further uses the heave-roll cross spectrum to estimate whether waves are incoming from port or starboard. When relevant, the algorithm also distinguishes between head and following sea. Further, Partial Least Squares Regression is used to estimate the significant wave height and the peak wave period. The algorithm is trained on a simulated dataset for NTNU's Research Vessel Gunnerus, and validated on a dataset with sea states not present in the training data. Results have been promising, and comparable to model-based methods with the same objective.

An online decision model has also been established. The model uses a Bayesian Belief Network which covers a range of factors which can affect the risk of collision for an autonomous ship. The model makes decisions based on the scenario/events present and the risk of collision at a point in time. Different scenarios have been tested in model experiments, where the system has shown to make the right decisions and take actions based on the scenario in question. The model is a good representation of an online and autonomous method using risk as the decision criteria, and can be further developed to include more scenarios and possible outcomes.

Sammendrag

Hovedtemaet i denne masteroppgaven er situasjonsforståelse. Oppgaven er todelt, hvor første del handler om sjøtilstandsestimering for et dynamisk posisjonert (DP) fartøy, og andre del handler om risikobaserte beslutninger for å unngå kollisjon for et autonomt DP fartøy. Begge temaene er i høy grad relatert til forskning om autonome skip, da sjøtilstand er en viktig input til et autonomt beslutningssystem.

En algoritme for sjøtilstandsestimering som er uavhengig av transferfunksjonene til skipet har blitt utviklet for et fartøy i DP. Algoritmen bruker Kvadratisk Diskriminant Analyse til å estimere den absolutte bølgeretningen, og estimerer videre om bølgen kommer fra styrbord eller babord ved bruk av hiv-rull krysspektet. Når det er relevant, skiller algoritmen mellom motsjø og medsjø. Videre bruker algoritmen Partial Least Squares Regression for å estimere signifikant bølgehøyde og bølgeperiode. Algoritmen trenes på et simulert datasett for NTNUs forskningsbåt RV Gunnerus, og er validert på data som ikke var i treningsdataen. Resultater har vært lovende, og sammenlignbare med modellbaserte metoder med samme mål.

En online beslutningsmodell har også blitt laget. Modellen bruker et Bayesiansk nettverk som dekker en rekke faktorer som kan påvirke kollisjonsrisiko for et autonomt skip. Modellen tar beslutninger basert på situasjonen og kollisjonsrisiko på et gitt tidspunkt. Forskjellige situasjoner har blitt testet i modelleksperimenter, hvor systemet tok riktige beslutninger og handlet basert på situasjonen. Modellen er en god representasjon på en online og autonom metode som bruker risiko som kriterie for å ta en beslutning, og kan bli utviklet videre til å inkludere flere situasjoner og utfall.

Preface

This master thesis was written in the spring of 2019, as the final delivery in the master program of Marine Cybernetics at the Department of Marine Technology.

The thesis is constructed as a collection of two scientific papers with a summary in the front. The first paper, *Sea State Estimation Using Quadratic Discriminant Analysis and Partial Least Squares Regression* has been submitted to the Joint CAMS and WROCO 2019. The second paper is called *Risk-Based Decision Making for Autonomous Ships: Collision Avoidance Case Studies*, and is to be submitted to the IEEE Control Conference. The work for this article has been done in close cooperation with Emilie Thunes.

Acknowledgements

Thank you to my supervisors Asgeir J. Sørensen and Ingrid B. Utne for all of their contributions to this master thesis. Asgeir has been motivating and able to help on all complications that have been encountered. Ingrid has given valuable input when developing the Bayesian Belief Network, and shared her competence for the production of the second article of this thesis. I would also like to thank my co-supervisors Astrid H. Brodtkorb and Børge Rokseth for all help. Astrid gave continuous support in the preliminary work throughout the fall of 2018, and has also been available for discussions and help during her maternity leave when I encountered problems. Her contributions and thorough proof-reading have been extremely valuable. Børge has been available on short notice throughout the spring. He has given crucial contributions for developing the decision model and valuable input to the second article of this thesis.

List of Abbreviations

AIS	**A**utomatic **I**dentification **S**ystem
ALARP	**A**s **L**ow **A**s **R**easonably **P**racticle
BBN	**B**ayesian **B**elief **N**etwork
CPSD	**C**ross **P**ower **S**pectral **D**ensities
DOF	**D**egree **O**f **F**reedom
DP	**D**ynamic **P**ositioning
EMLM	**E**xtended **M**aximum **L**ikelihood **M**ethod
GNC	**G**uidance, Navigation and **C**ontrol
GNSS	**G**lobal **N**avigation **S**atellite **S**ystem
GPS	**G**lobal **P**ositioning **S**ystem
HAZID	**Haz**ard **Id**entification
HAZOP	**Haz**ard and **Op**erabiliy Analysis
HIL	**H**ardware **I**n the **L**oop
IMU	**I**nertial **M**easurement **U**nit
JONSWAP	**Jo**int **N**orth **S**ea **Wa**ve **P**roject
PID	**P**roportional **I**ntegral **D**erivative
PLSR	**P**artial **L**east **S**quares **R**egression
PMS	**P**ower **M**anagement **S**ystem
QDA	**Q**uadratic **D**iscriminant **A**nalysis
RAC	**R**oot **A**utonomous **C**apabilities
RADAR	**Ra**dio **D**etection **A**nd **R**anging
RAO	**R**esponse **A**mplitude **O**perator
SCC	**S**hore **C**ontrol **C**enter
SJA	**S**afe **J**ob **A**nalysis
UAV	**U**nmanned **A**erial **V**ehicle
USV	**U**nmanned **S**urface **V**ehicle

Contents

Chapter 1

Introduction

Autonomous ships is a topic of increasing interest. The benefits of autonomous ships are many. To name a few, cost saving, human safety and efficient use of the vessel space are clear benefits of autonomy at sea (Brien, 2018). The common ground for all autonomous systems is the dependency on situation awareness. The system must be capable of processing information on the exact situation it is in and use it to make safe and effective decisions. This is also the case for a dynamically positioned (DP) vessel, which is an autonomous system capable of maintaining the vessel position and obtain the desired vessel position.

1.1 Motivation

The focus of this master thesis is how to use the data available for a DP vessel to increase situation awareness, and how to use the information about the situation to make decisions. Situation awareness does not only entail being aware of the surroundings in form of other constructions, but also aspects like weather, vessel motions and maintenance status. The weather is a crucial part of the vessel's awareness. Knowledge of the sea state has numerous applications, but specifically related to autonomy the main application is being an input into the decision system. For example, knowing the sea state can assist an autonomous system in decision making on whether the operation should continue, or if the risk of power loss or drift-off is high.

1.2 Main Contributions

The main contributions of this thesis are two papers. The first paper is on sea state estimation. The second paper is about risk-based decision making. Both are related to situation awareness, as the first article is about how to increase vessel situation awareness, and the second is about using the situation awareness to make decisions.

Paper A *Submitted to Joint CAMS and WROCO 2019*
A sea state estimation algorithm is developed, which uses the vessel response and non-model based methods to estimate the wave direction, significant wave height and peak wave period for a DP vessel. The methods used are Quadratic Discriminant Analysis (QDA) and Partial Least Squares Regression (PLSR). The algorithm successfully distinguishes between port and starboard waves, as well as head and following, and estimates the significant wave height and peak wave period with promising results. A simulation model developed at NTNU for Research Vessel Gunnerus is used to generate the dataset needed to train the sea state estimation algorithm.

Paper B *To be submitted to the IEEE Control Conference*
A Bayesian Belief Network (BBN) is constructed and used in an online decision model for an autonomous ship. The BBN covers factors like sensor failure, power failure and weather levels, and the end event is collision. A decision model is made, which makes decisions based on the scenario in question and the probability of a high risk of collision. Scenarios are simulated and tested in the laboratory, and the autonomous system successfully makes decisions and takes action. The vessel used is CyberShip Enterprise I and experiments were completed in NTNU's Marine Cybernetics Laboratory (MCLab).

1.3 Thesis Outline

The outline of the thesis is as follows:

- Chapter 2 covers autonomy aspects, which works as the bridge between the specific topics of this thesis. Status on autonomous ships, levels of autonomy, risk aspects and situation awareness are discussed.
- In Chapter 3, the background on sea state estimation is covered. Previous work is covered, as well as how to model waves and vessel response. The

chapter is concluded with some additional results from the sea state estimation algorithm presented in *Paper A*.

- Chapter 4 is related to *Paper B*. The chapter gives some background information on Hardware-in-the-Loop (HIL) simulations, presents HIL results, and describes the experimental setup for simulations and experiments.
- Chapter 5 concludes the thesis and discusses suggestions for further work.
- *Paper A* is called *Sea State Estimation Using Quadratic Discriminant Analysis and Partial Least Squares Regression* and proposes non-model based methods for estimating the sea state of a dynamically positioned vessel.
- *Paper B* is called *Risk-Based Decision Making for Autonomous Ships: Collision Avoidance Case Studies* and uses a BBN in a proposed decision system for an autonomous ship.

Chapter 2

Autonomy Aspects

The shipping industry is pursuing autonomous operations for various reasons. Shipowners would like to reduce operating cost (mainly related to crew, maintenance and fuel) and improve efficiency, offset skill shortages, as well as to further enhance safety. This chapter covers the aspects of autonomy – specifically motivation for introducing autonomous ships, how autonomy is defined, risk related to autonomy, and the importance of situation awareness.

2.1 Autonomy in the Shipping Industry

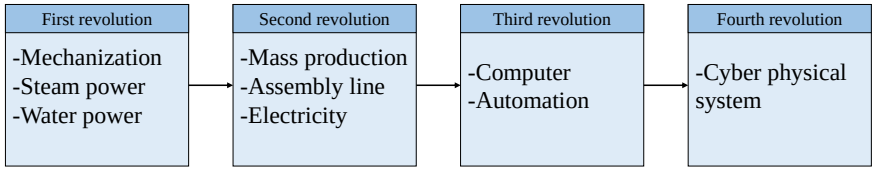

FIGURE 2.1: The four revolutions of the shipping industry (Lloyd's Register Group Ltd, 2017).

The four revolutions of the shipping industry are shown in Figure 2.1. With the fourth revolution in shipping, Shipping 4.0, the maritime industry is moving towards autonomy. This fourth step is enabled by a large share of processes on-board being computerized and automated, together with significant improvements in vessel connectivity and data availability. Automated and data-driven operations allow for moving tasks ashore into centralized hubs from where the vessel is operated either remotely or autonomously.

The field of autonomous ships is relatively mature. The world's first autonomous car ferry was successfully demonstrated in Finland during the fall of 2018 (Rolls-Royce, 2016). The vessel proved ability to avoid collision (using sensor fusion and artificial intelligence to detect objects) and perform autodocking (successfully changing speed and course when approaching the quayside and berth without human intervention). It also showcased a Shore Control Center (SCC), from where the vessel could be remotely operated if necessary.

Another example is YARA Birkeland, which will be the world's first fully electric and autonomous container ship. It is expected to be in operation by 2020 (Skredderberget, 2018), shipping products from two of YARA's production plants (Kongsberg, 2017). The vessel will start out with manned operations, then gradually become remotely operated and eventually fully autonomous. YARA Birkeland illustrates the potential of autonomous vessels in the short-sea shipping segment and their ability to compete with the cost of using trucks on voyages that are too short for traditional container vessels to be competitive. This is illustrated in Figure 2.2, as defined by Brinchmann (*Massterly: Autonomy in shipping; opportunities and challenges*).

Other examples within short-sea shipping is a project by Norwegian ASKO to transport equivalent of 16 trailers on a fully electric, autonomous ro-ro feeder, as well as the Seashuttle project by Samskip on a semi-autonomous container vessel trading between Norway, Sweden and Poland Brinchmann (*Massterly: Autonomy in shipping; opportunities and challenges*). Both the YARA and the ASKO project are aimed at commission operations in 2021.

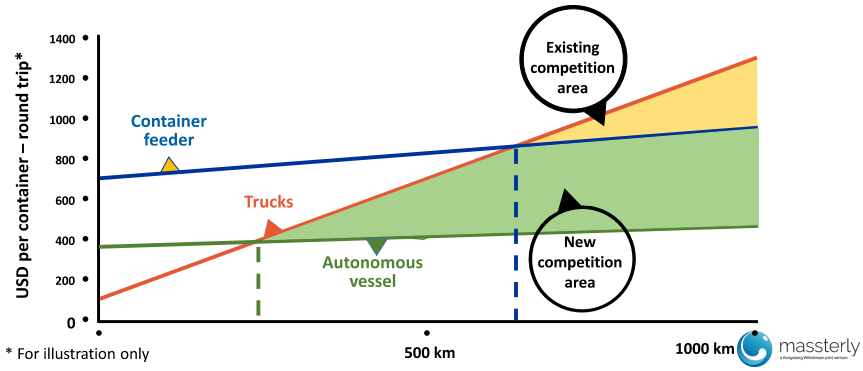

FIGURE 2.2: Competition areas between trucks and maritime shipping, for both a traditional container vessel and autonomous ships (*Massterly: Autonomy in shipping; opportunities and challenges*).

2.2 Levels of Autonomy

Generally, the required number of people for operating a ship in a safe and efficient manner depend on the vessel size, type and task, as well as how technologically advanced/equipped it is. With time, technology development has allowed for a gradual reduction in crew size. Today's diesel-electric propulsion requires a machinery crew of less than ten people. That is a major change from the coal-fired steam engines of the early 1900s, that needed a crew of several hundred people (*DNV GL: Remote-controlled and autonomous ships*). Increased autonomy implies reduced manning, thus reducing crew costs. However, autonomy requires large investments in technology. Especially where crew costs are low, there might not be a positive business case for investing in autonomy.

As vessels and their operations are getting more advanced, different skill-sets are required by their crew. Challenges with identifying and recruiting qualified personnel is another driver for shipowners to move towards autonomy (Lloyd's Register Group Ltd, 2019). A highly autonomous system may outperform a human in both efficiency and performance.

There are various definitions of the levels of autonomy. The International Maritime Organization (IMO) describe the degrees of autonomy (IMO, 2018) as:

- Degree 1: Ship with automated processes. The ship is navigated and controlled by humans, but some processes are automated.
- Degree 2: Humans are on board the ship, but the ship is operated remotely.
- Degree 3: No humans are on board, but ship is operated remotely.
- Degree 4: Fully autonomous. The system makes decisions and takes action without human interaction.

A DP vessel will typically be a degree 1 of autonomy ship, as the DP operation is automated but the vessel itself is humanly operated. Levels of autonomy can also be characterized by how involved humans are in decisions. As proposed in Sørensen (2013), the levels can be categorized as:

- *Automated system (Human in the Loop)*: Humans supervise all actions, but certain tasks and functions can be completed automatically.
- *Automated system - management by consent*: System gives recommendations to operator so the operator has time to decide on actions.
- *Semi-autonomous system - management by exception*: System makes own decisions when operator does not have time to make decisions. Operator can always override decisions made by the system.
- *Highly autonomous system (Human out of the Loop)*: System makes own decisions, can re-plan an operation, handle mistakes and reconfigure itself.

The technical requirements for achieving a fully autonomous ship are extensive. First of all, the vessel must be capable of doing its design tasks as good or better than a human would be, requiring a system with a broad understanding of the relevant operations, possible future events and handling of unexpected events. Additionally, the operation must be at least as safe as a humanly operated vessel, requiring the system to have knowledge of the safety on board as well as economic consequences related to different actions.

2.3 Risk Management

Another motivation for introducing autonomy is improving the safety level offshore by eliminating human exposure in operations. Removing personnel from hazardous situations is a major benefit of autonomy. However, unmanned vessels introduce other risk factors that need to be mitigated for, and autonomous vessels

must be at least as safe as traditional vessel. Risk for autonomous systems can be categorized using three aspects (Sørensen, 2013):

- Mission complexity
  - Complexity of the system's tasks, such as precision requirements, decisions and performance requirements.
  - Organization of and collaboration between participants in the operation.
  - Necessary performance, like quality of payload sensor data and control accuracy of vessel.
- Environmental complexity
  - Objects nearby.
  - Changing weather conditions.
  - Mobility constraints.
- Human independence
  - Level of autonomy.
  - Measure of how well the system perceives, analyzes, makes decisions and interacts.

Risk for an autonomous system can thus be defined by placing the score of the three aspects described above on a three-dimensional space as shown in Figure 2.3.

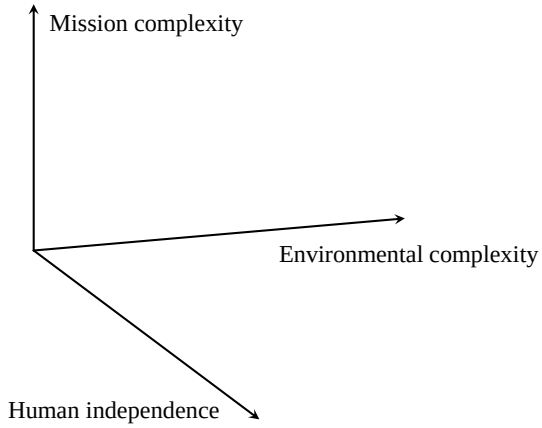

FIGURE 2.3: Axes describing how risk can be modeled for autonomous systems.

Huang (2007) states that insufficient measure in any of the factors listed above will reduce the safety level, in addition to insufficiency in any other Root Autonomous Capabilities (RAC). RACs are the system's ability to sense, perceive, analyze, communicate, plan, decide and execute (Huang, 2004). As the mission and environment becomes more complex, the safety level is reduced. This is because it requires a more complex and knowledgeable system. When human dependency is high, it adds the risk of human error, which often is the source of accidents.

Insurance, legal and approval aspects are among the challenges in the development of autonomous ships. Regulatory challenges arise as there are new risks introduced. This is due to both cyber- and physical security of the vessel, but also due to the technical dependencies of the system. A single technical failure in a system of an autonomous or unmanned vessel may have serious consequences. With the amount of possible events that can occur, the regulatory requirements for testing and verification need to be extensive(*Teknologien endrer samfunnet* 2018).

As mentioned above, an important risk aspect related to autonomy, is the possibility of cyber attacks. Maritime Unmanned Navigation through Intelligence in Networks (MUNIN) is a collaborative research project, co-funded by the European Commissions. They aim towards a concept of an autonomous ship (MUNIN, 2016). In an assessment by the MUNIN project, Kretschmann (2015), it is stated

that the risks ranked highest are jamming, spoofing or hacker attacks of the Automatic Identification System (AIS), Global Positioning System (GPS) signals, or communication systems. If there is a crew on-board the vessel, it is assumed that control of the vessel can be regained in case of an attack by the crew turning off external dependencies. However, with an unmanned vessel this will be impossible and reaching the vessel physically before the damage is done can prove difficult (Vinnem et al., 2018). Such attacks could lead to grounding or collision, potentially with a ship with passengers or large amounts of oil. However, the vessel on the collision course of a hacked vessel will in most cases be able to maneuver away from collision, so the real threat is actually for infrastructure. Bridges, open sea areas, and offshore oil and gas installations are all examples of infrastructure which would be unable to move to avoid collision (Vinnem et al., 2018), where all are likely to have fatal effects. This is just another aspect contributing to the difficulties of classifying and verifying autonomous ships.

Complex operations with a high risk require a detailed operational procedure. An operational procedure includes the sequential steps like mobilization, testing, transiting, launching, mapping recovering and demobilizing (*Teknologien endrer samfunnet* 2018). With an operational procedure, the DNV GL recommendations for managing risk should be followed. A simplified version of the model can be seen in Figure 2.4.

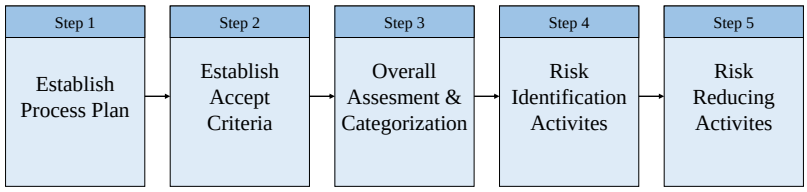

FIGURE 2.4: Simplified version of DNV GL's five step model for managing risk (DNV GL, 2017).

Step two in Figure 2.4 entails establishing which criteria are acceptable. The common criteria is As Low As Reasonably Practical (ALARP), defined as "a level of risk that is not intolerable, and cannot be reduced further without the expenditure of costs that are grossly disproportionate to the benefit gained" (Rausand, 2011).

In step three and four in Figure 2.4, Hazard Identification should be done (HAZID). The purpose of HAZID is to identify hazards at an early stage to assist in choosing advantageous procedures or design. A hazard will lead to a

hazardous event unless precautions are taken and hazards related to a particular operation must therefore be identified (DNV GL, 2017).

In step four, one should also complete a Hazard and Operability Analysis (HAZOP) and Safe Job Analysis (SJA). HAZOP uses experts to conduct analyses of a system to explore hazards. SJA analyzes activities to establish preparedness and risk management. In step five of the risk management model, risk mitigating measures are identified.

2.4 Situation Awareness

Situation awareness is the basis for nearly all aspects related to autonomous ships. The vessel's awareness of the surrounding objects, objects on its collision course, the weather, vessel motions and maintenance levels on machinery and hull cover a range of the factors an autonomous ship should be aware of. The quality of the control system has little impact if the data on the current situation is unavailable.

This section covers previous work on situation awareness, as well as a subsection on how situation awareness is obtained and situation awareness for a DP operation.

2.4.1 Previous Work

Situation awareness is of interest not only for autonomous or unmanned ships, but for all seafaring. It is important for underwater vehicles, ships navigating in harbours, ships on crossing courses and DP operations to name a few.

Clemente et al. (2014) propose a collision avoidance system which applies a cognitive situation awareness framework. The framework is comprised of the general Endsley model for situation awareness, as well as data management activities, semantic technologies and uncertainty methods. The Endsley model for situation awareness has three levels: perception, comprehension and projection (Endsley, 2000). Perception entails observation of important information, while comprehension entails understanding and combining this important information. The third level, projection, is the ability to forecast future events, allowing for decision making. A visualization of this model is shown in Figure 2.5, showing how different factors influence the situation awareness, and thus the decision and performance of a system.

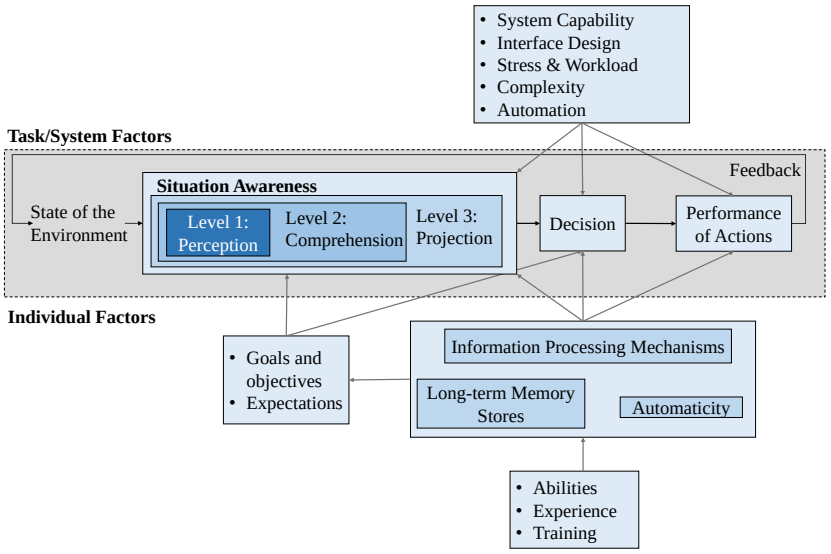

FIGURE 2.5: Endsley model for situation awareness. Inspired by Endsley (1995).

Clemente et al. (2014)'s extension of this model specifically involves the integration of Semantic Sensor Network Ontology to represent sensor information and manage uncertainties from the sensor network. Cognitive maps to evaluate the potential evolution of current events are also proposed.

Porathe et al. (2014) investigate what information is necessary for an onshore control centre to acquire adequate situation awareness for an unmanned ship. The paper proposes the necessary information groups to obtain situation awareness, found using a focus group. The list of information groups include

- Voyage, i.e. the voyage plan.
- Sailing: position, course and other standard information usually found on the bridge.
- Observations. This includes information from the object identification system such as Radio Detection and Ranging (RADAR) and AIS.
- Safety and emergencies which includes information on firefighting, water ingress etc.
- Security. Security sensitive log-on to the vessel information, as unmanned vessels are sensitive to cyber attacks. Also to keep track of things like door status, personnel on board, and possible intruders.

- Cargo, stability and strength. This information group contains information on the stability systems and tank levels.
- Technical, tracking the engine control system.
- SCC, containing things the vessel is unable to handle such as voice communication.
- Administrative: crew lists and such.

Porathe et al. (2014) also recognize that one of the main challenges in autonomous navigation is extreme weather. In extreme seas, the autopilot is often turned off and it is the captain's experience and situation awareness that are able to slow down at the correct point in time, or alter the course. Obtaining these same feelings for an operator on shore is challenging, but hopefully possible with gyro stabilizing cameras. Another challenge is for the autonomous system to alert the SCC when its performance is not satisfactory.

Andrade et al. (2017) suggest and present results of using an Unmanned Aerial Vehicle (UAV) to map the area near the vessel to give the captain an overview of the surroundings and warn about upcoming obstacles on the vessel path. Results showed that the UAV successfully followed the planned path of the ship. Although this study is not for an autonomous ship, the concept may be valuable in achieving high situation awareness for an autonomous ship and for the land-based operator.

2.4.2 Obtaining Situation Awareness

A manned and an autonomous vessel gain situation awareness in many of the same ways. They both rely on sensor data, although an autonomous vessel to a much higher extent. With a manned vessel, sensor errors can often be managed by the personnel on board, which may not be the case for an autonomous vessel. This chapter therefore covers some background info on the sensors and data that must be available for an autonomous vessel.

Liu et al. (2016) propose the elements comprising an Unmanned Surface Vessel (USV):

- The hull.
- Propulsion and power system, usually a rudder and propeller providing steering and thrust.

- Guidance, Navigation and Control (GNC) system. GNC is a crucial component, usually composed of computers and software.
- Communication systems, which do not only include wireless communication with onshore and other vessels, but also communication between the different systems and sensors on-board.
- Data collection equipment. This is crucial to be able to gain situation awareness. Sensors include Inertial Measurement Unit (IMU), Global Navigation Satellite System (GNSS), cameras, RADAR, AIS and LIDAR.
- Ground station. This is where missions are received from.

Situation awareness cannot be obtained without sensor data. A short description of each sensor's role follows:

IMU: The IMU typically has measurements from three-axes rate gyros, accelerometers and magnetomoeters. A gyroscope detects rotation using the concept of momentum conservation. Accelerometers measure acceleration, and are either mechanical or based on frequency shifts due to increased tension in a string. Magnetometers are used to find the compass heading and roll-pitch angles (Fossen, 2011). Measurements from the IMU, are for example crucial for a sea state estimation algorithm based on the vessel response, providing increased situation awareness of the surroundings.

GNSS: The purpose of the GNSS is to provide a position reference. GNSS systems include the GPS from the United States, and the GLObal'naya NAvitsionnay Sputnikovaya Sistema (GLONASS) from Russia. These systems can be assisted by the more recent and accurate GALILEO positioning system, a system by the European Union . The position of a marine vessel is usually measured with differential GNSS, which involves a fixed receiver, for example on shore with known position, used to calculate the GNSS position errors. The errors are then transmitted to the ship and used as corrections for the actual position (Fossen, 2011).

Camera: Both thermal imaging and high definition visual cameras can be used to detect objects (Advanced Autonomous Waterborne Applications (AAWA), 2016). Prasad et al. (2016) discuss the challenges involved in video based object detection at sea, and state that challenges include the dynamic nature of the background, small distant objects and illuminating effects.

RADAR: The purpose of the RADAR is to detect the location of an object, and the distance from the vessel that this object is located. The object is detected by transmitting a radio energy pulse, which is reflected by the potential object. The time spent from the pulse being sent to being received back, as well as the speed

of the signal, is used to calculate the range of the target. To be able to detect the direction from the vessel in which the object is located, a single antenna is used for both transmission and reception, assuring that energy is transmitted in a narrow beam in the horizontal plane (Bole, 2005).

AIS: The AIS contains three types of information: dynamic data such as position, course and speed, static data like identity, vessel type, dimensions, and lastly the details on the sailing such as destination, estimated time of arrival, cargo and draught (Norwegian Coastal Administration, 2016).

LIDAR: LIDAR has similar applications as RADAR, where the difference is that LIDAR uses light instead of radio pulses. LIDAR is said to be more accurate than RADAR, but unlike RADAR, LIDAR will be negatively affected by weather like rain and fog. LIDAR technology is also more expensive than RADAR, but can work over longer distances. LIDAR is more angularly accurate than RADAR (Rothman, 2018).

All of the sensors described above will in their own way provide information contributing to an autonomous vessel's situation awareness. Although sensor technology is developing fast, the sensors all have limitations. The AIS will for example not be able to detect all the smaller vessels, and the LIDAR is limited by weather. With a fusion of the data from high-technology sensors, the goal is to be able to have redundancy on information and reduce the probability of a system receiving false or lacking information. Additionally, interpreting the data is another challenge in achieving situation awareness. The system must be capable of using the information to determine if a situation is hazardous or not. The margins may be small, and differentiating between a safe and unsafe situation may be challenging for a computer system.

2.4.3 Situation Awareness in Dynamic Positioning

Øvergård et al. (2015) discuss the situation awareness of DP operators, and demonstrate results from interviews with operators after incidents occurred. This section is based on information and results from Øvergård et al. (2015), and the purpose is to demonstrate some of the DP operators responsibilities, which one day will be an autonomous system's responsibility.

The research is based on the three level Endsley model for situation awareness, described in Section 2.4.1. 24 different work situations were studied, where the

situation awareness level of each situation was established. The interviewed operators differed in age and experience, but all had been involved in a critical incident as a DP operator. Critical incidents were defined as non-routine happenings with a high damage potential. Base events, or initiating events were:

- Environmental impacts.
- Power Management System (PMS) error.
- Human error.
- DP reference system problem.
- Component failure.
- DP software problem.

The operators informed that the most important mitigating measures were to secure the gangway, to protect people, and stop the vessel from colliding in the offshore installation. In 14 out of the 24 events, level 1 situation awareness was not obtained, meaning the operators only became aware of the base event after the event. In 19 of the 24 incidents, level 2 situation awareness was obtained as the operator was able to understand the relevance of some information. Level 3 situation awareness was only obtained five times, and operators were hence surprised when the incident occurred in the remaining 19 cases. The consequences of these events were drive off, drift off, force off, being on a collision course or keeping position.

The study presented above demonstrates the extent of situation awareness that an autonomous DP vessel must have. The operator's situation awareness and risk assessment was based on perception of cues, what they expected to happen, problem and goal identification, limitations related to time, and uncertainty in recognizing the based events, which are all tasks that an autonomous system need to perform equally well, preferably better.

Chapter 3

Background on Sea State Estimation

This chapter covers previous work within the field of sea state estimation. This is followed by a section on how waves are modeled, and how these result in vessel motions. Further, brief information on how the dataset used to train the sea state estimation algorithm is described. Lastly, some additional results from the sea state estimation algorithm formally presented in Arneson et al. (2019) (*Paper A* appended to this thesis) are shown and discussed.

3.1 Previous Work

Previous work on sea state estimation go back to the 1970s. On-site monitoring systems and decision support systems needed estimates of the sea state at the actual position of the vessel, recognizing the need for sea state estimation (Nielsen, 2017). Studies on sea state estimation have been conducted for vessels with and without forward speed, in both the frequency and time domain, and have been both parametric and non-parametric. Parametric methods assume the wave spectrum to be a parametrized wave spectrum, and non-parametric methods find the wave spectrum without prior knowledge of its shape (Nielsen, 2006).

Early studies for a dynamically positioned vessel were done by Pinkster (1978). The study investigates the use of wave feed-forward to improve dynamic positioning, and the wave height is estimated by measuring the wave height at a discrete, finite number of points using wave probes. The method assumes that the relative wave height does not vary rapidly with position around the vessel's waterline.

Later, several attempts were made for sea state estimation for vessels with forward speed. The first to strictly consider the Doppler shift was Iseki et al. (2000) (Nielsen, 2017). The Doppler shift occurs when the vessel has forward speed, as the encounter frequency between the waves and the vessel needs to be considered. In following sea, there are three true wave frequencies contributing to the power spectrum at certain encounter frequencies. In practice this means that the measured cross spectra consist of a sum of three terms where the directional wave spectra are different in the different terms (Iseki et al., 2000). The method in Iseki et al. (2000) further proposes a Bayesian model for estimating the directional wave spectra, based on a modelling procedure proposed in Akaike (1980). This procedure consists of finding unknown coefficients by maximizing the product of the likelihood function and the prior distributions. A prior distribution can be thought of as a stochastic constraint and a character of the model which is known.

A parametric sea state estimation method is proposed in Nielsen et al. (2012). The chosen spectrum is a 15-parameter tri-modal spectrum, which accounts for mixed sea such as wind and swell. The method is based on the so-called wave buoy analogy, and uses the equation relating the measured cross spectrum and the estimated cross spectrum. The estimated cross spectrum is calculated using the transfer function, the Response Amplitude Operator (RAO) and the calculated cross spectrum. This is then considered an optimization problem, minimizing the difference between the estimated and calculated spectrum, yielding an estimated wave spectrum and thus the sea state.

Studies have also been extensive on sea state estimation for DP vessels. Waals et al. (2002) propose a method which estimates the directional wave spectrum based on measurements from six relative wave height sensors. These measurements were used to to find the Cross Power Spectral Densities (CPSD), and the Extended Maximum Likelihood Method (EMLM) minimizes the difference between the measured and theoretical CPSD. The theoretical CPSD is a geometrical phase difference and normalized transfer functions of the relative wave height. Non-parametric methods for sea state estimation for a DP vessel are also presented in Tannuri et al. (2003) and Pascoal et al. (2008).

3.2 Modelling Waves

This section is based on information from Faltinsen (1990). The wave surface elevation, as a function of space and time, for long-crested irregular sea propagating

in the positive x-direction can be presented as a sum of many regular wave components :

$$\zeta(x,t) = \sum_{n=0}^{N} \zeta_{A_n} cos(\omega_n t - k_n x + \epsilon_n) \tag{3.1}$$

ζ_{An} is the wave amplitude, ω_n is the wave frequency and k_n is the wave number, defined as $\omega_n^2 = gk_n$ for deep water. ϵ_n is the random phase angle which is rectangularly distributed between 0 and 2π.

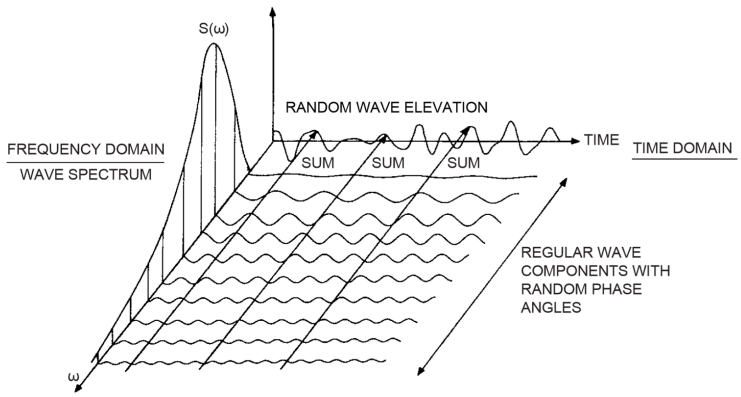

FIGURE 3.1: Connection between time and frequency domain for long-crested short-term sea (Faltinsen, 1990).

The instantaneous surface elevation, ζ in (3.1) at t = 0, is normally distributed around zero. Figure 3.1 shows a graphical illustration of the relationship between the time and frequency domain, as it shows many regular wave components and how they sum up to the wave elevation. It can also be seen in Figure 3.1 that $\zeta(x,t)$ has an associated spectrum as a function of frequency, denoted $S(\omega)$. The area under the curve in a frequency interval represents the total energy in the wave components in this frequency range. The surface elevation and wave spectrum are related through the equation below.

$$\frac{1}{2}\zeta_{A_n}^2 = S(\omega_n)\Delta\omega \tag{3.2}$$

When estimating the sea state, the interesting outputs are the significant wave height, peak wave period and wave direction. Significant wave height, H_s, is the average of the 1/3 largest wave heights, usually in a three-hour time interval. Both the significant wave height and peak wave period can be obtained from a wave spectrum.

The standardized wave spectrum called the Joint North Sea Wave Project (JONSWAP) spectrum is used to model waves in the simulation model used for the sea state estimation algorithm in the appended *Paper A*. The JONSWAP spectrum can be obtained from a Rayleigh distribution, which assumes a narrow-banded spectrum and a Gaussian distributed instantaneous surface elevation. The JONSWAP spectrum is most applicable in the sea state range where $3.6 < T_p/\sqrt{H_s} < 5$ (DNV GL, 2007).

Figure 3.2 shows the JONSWAP wave spectrum for $H_s = 4$ m and $T_p = 8$ s. One of the parameters determining the shape of the JONSWAP spectrum, and what in fact separates it from a Pierson-Moskowitz spectrum, is the non-dimensional peak shape factor, γ. Figure 3.2 shows the spectrum for two different γ-values, showing that higher γ values increase the peak spectral value, and thus the energy in the sea state around the peak frequency.

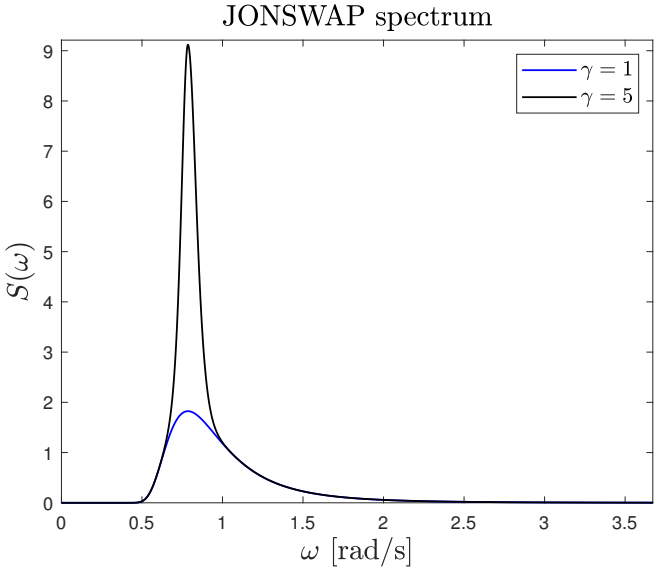

FIGURE 3.2: JONSWAP spectrum for $H_s = 4$ m. and $T_p = 8$ s., showing the spectrum for two different non-dimensional peak shape parameters.

3.3 Response Spectrum

Linear wave theory can to a large extent describe wave-induced motions for structures at sea. However, at high sea states the nonlinear effects' contribution is

large, and should be considered. Linear theory in practice means that in non-steep waves, the wave-induced motions are linearly proportional to ζ_a.

R_{ij}, $i, j = \{z, \phi, \theta\}$ is the complex valued cross-spectra for heave, roll and pitch and is given by

$$R_{ij}(\omega) = X_i(\omega, \beta)\overline{X_j(\omega, \beta)}S(\omega) \tag{3.3}$$

where β is the relative direction of the wave. $X_i(\omega, \beta)$ is the complex-valued motion transfer function, which provides the motion amplitude per unit incident wave amplitude, as well as the phase of the motions relative to the waves. $\overline{X_j(\omega, \beta)}$ is the complex conjugate of the transfer function, the so called RAO, giving the response amplitude per unit incident wave amplitude (Greco, 2012).

In addition to the significant wave height and peak wave period, the direction of the incoming wave also largely affects the response of the vessel. This is clear from (3.3) as the transfer function, $X_i(\omega, \beta)$, depends on the wave direction, β. The wave direction is defined as 180° when incoming straight on the bow (head sea), and 0° when incoming from stern (following sea), as shown in Figure 3.3. The wave direction is negative when incoming waves are from the vessel starboard side.

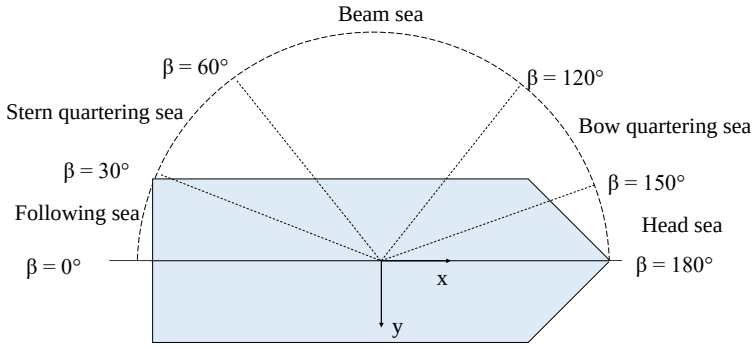

FIGURE 3.3: Relative wave directions.

3.4 Generating Data for Sea State Estimation

The dataset used to train the sea state estimation algorithm was generated using an existing MATLAB/Simulink model, developed at NTNU.

The model consists of an environmental module, marine vessel module and a control system, connected as presented in Figure 3.4.

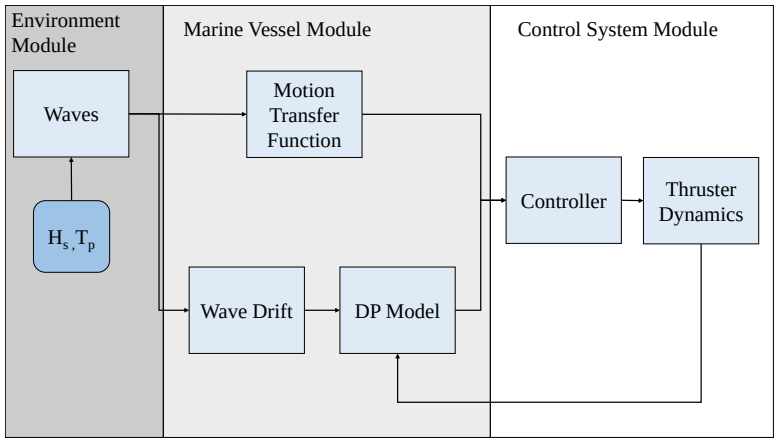

FIGURE 3.4: Block diagram of the simulation model used for data generation to train the sea state estimation algorithm.

The environmental module models waves based on H_s and T_p, in correspondence with the wave modeling theory described in Section 3.2. The motion transfer function is used to obtain the wave-frequency motions. These consist of frequency-dependent added mass forces, vessel's mass and moment of inertia, wave radiation damping and restoring due to gravity and buoyancy. The wave drift block calculates the 6 Degree of Freedom (DOF) wave-frequency excitation forces on the vessel using its force transfer functions. The DP model block contains the equations of motion, and finds the low-frequency motions. The low-frequency forces consist of inertial forces, Coriolis and centripetal forces, damping and current forces, restoring forces, environmental forces and thruster forces (Sørensen, 2013). The total motion of the vessel is a sum of the low-frequency and wave-frequency motions. The commanded thruster forces in the simulation model are computed using a Proportional Integral Derivative (PID) controller for DP, and are allocated to the thrusters in the thruster dynamics block.

To generate the dataset each sea state was simulated for 12 minutes. This is to assure that steady state has been reached. The time series of the vessel response in all DOFs for each sea state were transformed to the frequency domain using the Fourier transformation. To obtain a single value for each DOF for the particular sea state, the frequency domain response was integrated over the frequency range. The results are then one response value for surge, sway, heave, roll, pitch and yaw for every sea state. These values, as well as the significant wave height, peak

period and wave direction were recorded and used as training data to develop the sea state estimation algorithm.

3.5 Additional Results

This section shows some results from the sea state estimation algorithm in Arneson et al. (2019) (*Paper A* in the appended papers) that are not shown in the article. Specifically, the resulting regression coefficients from PLSR will be shown and discussed.

As the vessel response largely depends on the direction of the incoming waves, the algorithm needs to consider the wave direction when estimating the sea state based on the vessel response. That is why the algorithm firstly estimates the wave direction, and further chooses the regression coefficients for that particular wave direction. The coefficients for H_s and T_p are shown in Tables 3.1 and 3.2 respectively. The color scale is darker for higher absolute values, i.e. darker for the DOFs with high contributions in the calculation of H_s or T_p. For a time series of motions, each DOF has a preprocessed value and the regression coefficients represent the weight of these values in the calculation of H_s and T_p.

TABLE 3.1: Regression coefficients for H_s.

Wave direction	Surge $\cdot 10^4$	Sway $\cdot 10^4$	Heave $\cdot 10^4$	Roll $\cdot 10^4$	Pitch $\cdot 10^4$	Yaw $\cdot 10^4$
0°	4.9	0.0	2.0	0.0	-16.3	0.0
30°	3.0	5.0	0.5	14.4	-3.2	-0.4
60°	0.8	4.8	0.7	8.0	-0.7	-0.4
90°	0.0	3.7	2.1	-1.5	-0.1	0.0
120°	1.7	4.3	0.9	3.6	-2.6	-1.0
150°	2.1	3.3	2.8	-3.1	-5.2	-1.6
180°	3.9	0.2	1.9	0.0	-14.6	0.0

TABLE 3.2: Regression coefficients for T_p.

Wave direction	Surge $\cdot 10^4$	Sway $\cdot 10^4$	Heave $\cdot 10^4$	Roll $\cdot 10^4$	Pitch $\cdot 10^4$	Yaw $\cdot 10^4$
0°	-0.8	0.0	0.4	0.0	12.4	0.0
30°	-0.2	0.1	0.0	1.1	-0.3	0.0
60°	-0.1	-0.1	0.0	0.3	0.0	0.0
90°	0.0	-0.1	0.0	0.4	0.0	0.0
120°	-0.1	-0.1	0.0	0.3	-0.3	-0.1
150°	0.1	-0.4	0.0	0.7	1.1	0.3
180°	-0.1	0.0	-0.1	0.0	3.1	0.0

As can be seen in both tables, the roll and sway motions contribute close to nothing in head and following sea. Similarly, surge and pitch are not important motions in beam sea. Surge, heave and pitch are the important motions in head and following sea, and the effect of these gradually decrease when moving to quartering and beam sea. The roll and sway motions have their maximum contributions in stern quartering sea in the H_s-regression, and in bow quartering sea for the T_p-regression.

Chapter 4

Simulations and Experiments

The chapter covers some background on HIL testing and its applications, and further shows the HIL simulation results produced in relation to the testing of the risk-based decision model proposed in *Paper B*. The experimental setup for HIL simulations and model experiments is also covered at the end of this chapter.

4.1 Background on Hardware-in-the-Loop

In the movement towards autonomous ships, the need for reliable approaches for verification of control systems increases. This is to ensure that performance and safety requirements are met. Verification and testing early in the process is efficient and cost saving (Kapinski et al., 2016).

One such approach is HIL testing. Before conducting model experiments to test the decision model performance, HIL-tests were performed to verify the system. In HIL-testing, the system consists of a real-time platform and a virtual plant. The virtual plant can either run in real time on specialized hardware, or a combination of a computer model and physical components (Kapinski et al., 2016).

In the case of a marine system, the hardware should be capable of simulating the dynamic response of the vessel and should contain sophisticated models of the vessel and its equipment (DNV GL, n.d.). The HIL simulator realistically imitates the vessel systems and the environment and responds to the control demands. This process is illustrated in Figure 4.1. From the control system point of view, its inputs are the same as in the real world, and HIL testing therefore facilitates systematic testing of performance, functionality, control system and error handling.

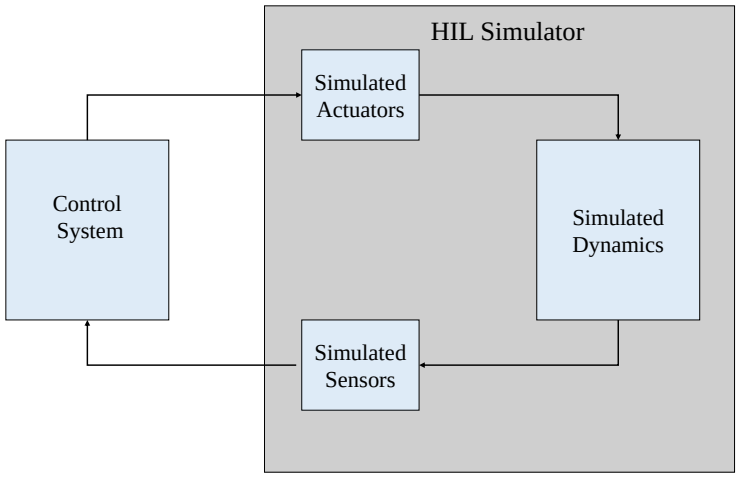

FIGURE 4.1: Concept of HIL-testing. Figure inspired by DNV GL (n.d.).

4.2 Hardware-in-the-Loop Results

In the second appended paper, experimental results are shown for three chosen scenarios, to demonstrate the decision model performance. Before these experiments were conducted, the decision model performance was checked in HIL-tests. This section shows these results for the three scenarios. These scenarios and the decisions the vessel makes are further described in *Paper B*, but the figure captions briefly explain the events.

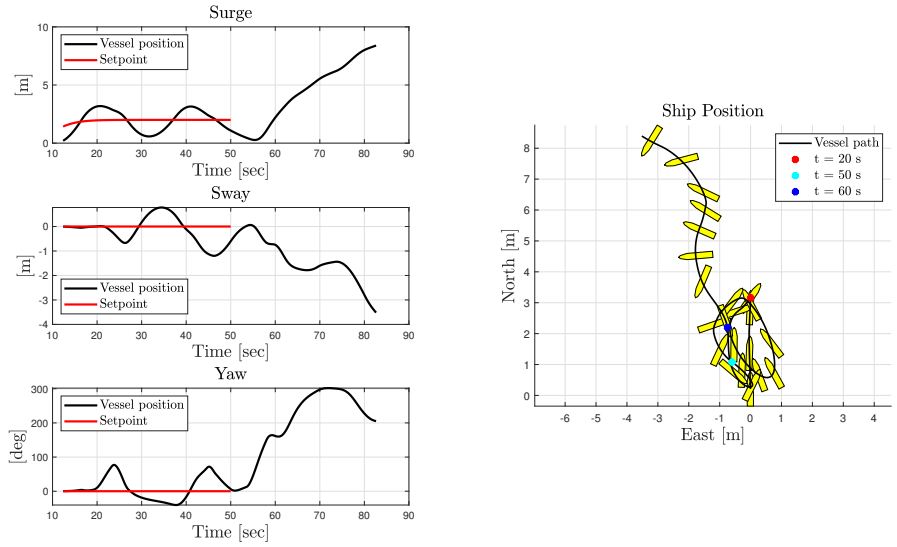

FIGURE 4.2: HIL simulation results for scenario 1. Position in surge (upper), sway (middle) and yaw (lower) are shown, as well as vessel path (right). Vessel is manually maneuvered from t= 50 s. and onward, as the vessel situation awareness has been lost.

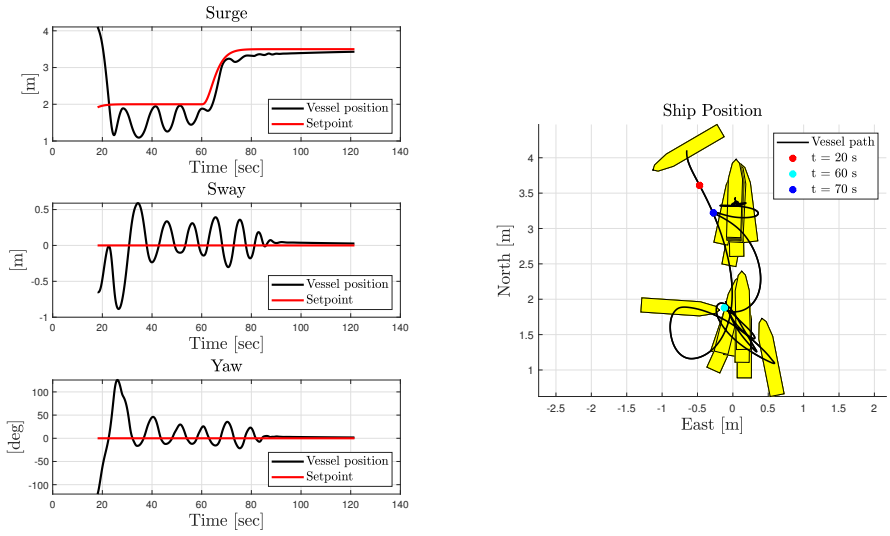

FIGURE 4.3: HIL simulation results for scenario 2. Position in surge (upper), sway (middle) and yaw (lower) are shown, as well as vessel path (right). Setpoint is changed at t = 50 s., as the weather is extreme and maintenance has been unsatisfactory.

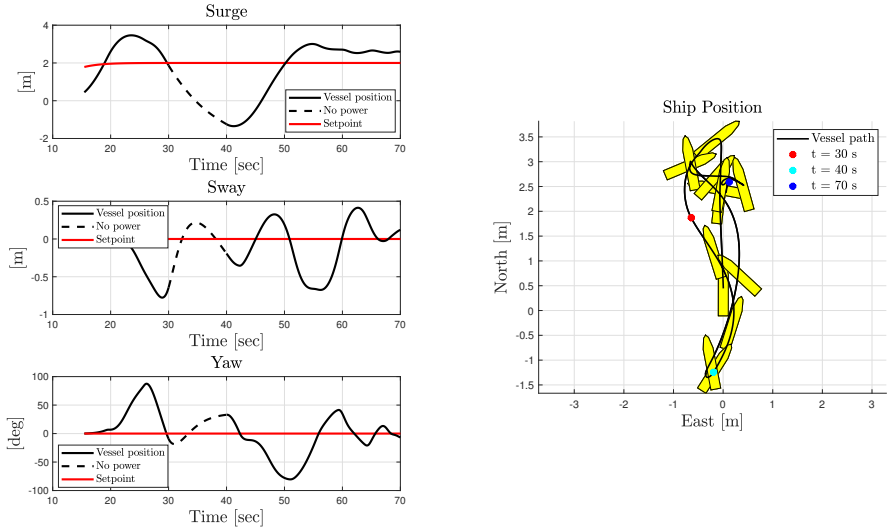

FIGURE 4.4: HIL simulation results for scenario 3. Position in surge (upper), sway (middle) and yaw (lower) are shown, as well as vessel path (right). Power is lost at t= 30 s. and regained at t = 40 s.

As is seen from the results, the vessel follows its setpoint (except when manually maneuvered). Results showed satisfactory performance, such that the model was tested further in model experiments.

4.3 Experimental Setup

This section is written in cooperation with Emilie Thunes, co-author on *Paper B*. The section covers background information on the vessel used in experiments, CS Enterprise I, as well as information on the hardware and software necessary to perform the HIL-simulations and model experiments. The chapter is mainly based on information from *CyberShip Enterprise I User Manual*. All experiments were performed in the MCLab basin at NTNU.

4.3.1 CS Enterprise I

The CS Enterprise I vessel is 1:50 scale tug boat, equipped with one bow thruster (BT) and two Voith Schneider propellers (VSP). The vessel is illustrated in Figure 4.5, with corresponding dimensions shown on the figure and in Table 4.1 The model ship is used during full scale testing of the maneuvering control design, PID controller and decision model.

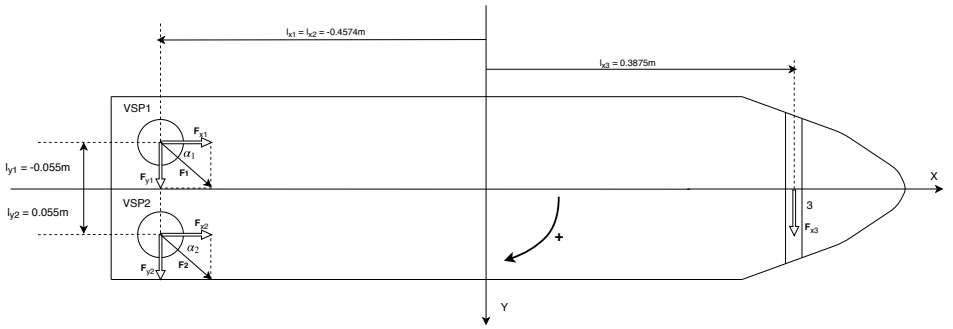

FIGURE 4.5: Thruster placement on CS Enterprise I

TABLE 4.1: Dimensions of CS Enterprise I

LOA	1.105 [m]
B	0.248 [m]
Δ	14.11 [Kg]

The low-speed control design model of CS Enterprise I is given by

$$\dot{\eta} = R(\psi)\nu \tag{4.1}$$

$$M\dot{\nu} = -C(\nu)\nu - D(\nu)\nu + \tau \tag{4.2}$$

where η is the surge, sway and yaw position vector and ν is the surge, sway and yaw velocity vector. $R(\psi)$ is the rotation matrix, M is the vessel inertia matrix, $C(\nu)$ is the coriolois and centripetal matrix and $D(\psi)$ is the damping matrix. M and $C(\nu)$ are dependent on the rigid body and hydrodynamic added mass parameters, as well as hydrodynamic damping parameters. $D(\nu)$ is a function of the hydrodynamic damping parameters. The necessary coefficients are given in Tables 4.2 an 4.3.

TABLE 4.2: CS Enterprise I rigid body and added mass parameters

Rigid body		**Added mass**	
Parameter	**Value**	**Parameter**	**Value**
m	14.11	$X_{\dot{u}}$	-2.00
I_z	1.76	$Y_{\dot{v}}$	10.00
x_g	0.04	$Y_{\dot{r}}$	-0.00
y_g	0.00	$N_{\dot{r}}$	-1.00

TABLE 4.3: CS Enterprise I damping parameters

Surge		**Sway**		**Yaw**	
Parameter	**Value**	**Parameter**	**Value**	**Parameter**	**Value**
X_u	-0.66	Y_v	-1.33	N_v	0.00
X_{uu}	0.35	Y_{vv}	-2.78	N_{vv}	-0.21
X_{uuu}	-3.79	Y_{vvv}	-64.91	N_{vvv}	0.00
X_v	0.00	Y_r	-7.25	N_r	-1.90
X_{vv}	-2.44	Y_{rr}	-3.45	N_{rr}	-0.75
X_{vvv}	0.00	Y_{rrr}	0.00	N_{rrr}	0.00
–	–	Y_{rv}	-0.81	N_{rv}	0.13
–	–	Y_{vr}	-0.84	N_{vr}	0.08

4.3.2 Hardware Architecture

The model ship is powered with a 12V12Ah battery on-board. The battery is mounted by connection of the positive and negative terminal to the vessel using wires. In addition, CS Enterprise I is equipped with an IMU from Analog Devices. The sensor type is ADIS16364, which includes a triaxis accelerometer and gyroscope. The coordinate frame of the IMU is left-hand orientation for linear accelerations and right-hand orientation for the angular rates. This is accounted for by multiplying the accelerations with -1. The control system on-board the scale model consists of four parts:

Compact re-configurable input/output (cRIO): cRio is an embedded controller provided by National Instruments. The ship model is equipped with the cRIO-9024 version, which is an embedded real-time controller, commonly used for advanced control and monitoring. The cRIO-90234 reads positioning data and is connected to four Field Programmable Gate Array (FGPA) modules for I/O.

- NI-9215: Used for measuring voltage.
- NI-9263: Used for reading IMU measurements.
- NI-9401: Not used.
- NI-9474: Used for sending Pulse-Width-Modulated (PWM) signals.

Raspberry Pi (RPi): The RPi provides the communication with the Sixaxis controller. The Sixaxis controller transmits information from the joystick to the RPi. This is accomplished by Bluetooth communication. When the RPi is powered, it starts searching for a wireless controller. As soon as the RPi is successfully connected to a controller, the controller will output commands through the Ethernet to the cRIO.

Electronic Speed Control (ESC): The ESC controls the thruster motor speeds. These are controlled with PWM signals from the cRIO.

Four servos: The servos control the position of the VSP steering rods.

In addition to the on-board control system, a laptop is used in the communication system. The laptop reads simulated data and sends inputs to the cRIO based on outputs from the VeriStand Engine. The inputs are sent over the MCLab Wi-Fi. An illustration is displayed in Figure 4.6. Additional information is found in Marine Cybernetics laboratory handbook (*Marine Cybernetics Laboratory Handbook* 2017).

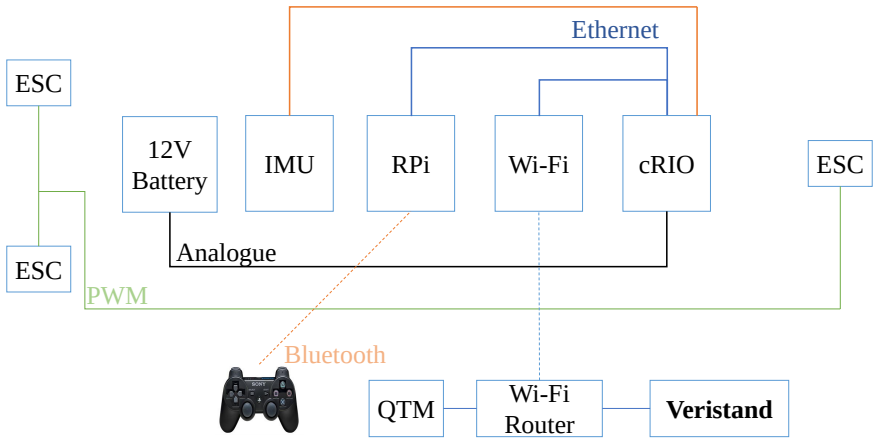

FIGURE 4.6: CS Enterprise hardware setup

4.3.3 Software Architecture

Several software parts are needed in order to utilize the hardware architecture from section 4.3.2. This includes the MATLAB/Simulink system, the VeriStand software and the Qualisys Track Manager (QTM) software.

The MATLAB/Simulink system is developed at NTNU, and can be downloaded from GitHub. The different models include ctrl_custom, ctrl_DP, ctrl_sixaxis2thurster and u2.pwm, where ctrl_custom is the model modified and used for this thesis. Figure 4.7 shows a block diagram of the elements in ctrl_custom, along with the elements added to facilitate for risk-based decision making. A PID controller has been developed, which takes inputs from the observer and a reference model. The reference model smoothens the vessel setpoint to a realistic vessel path. The actuator system gets the commanded thrust from the PID, and communicates the allocated thrust to the plant. The plant models the vessel position, which is estimated by a sensor system. These noisy sensor measurements, along with the commanded thrust, are used in a Nonlinear Passive Observer (NPO) which produces estimated vessel positions.

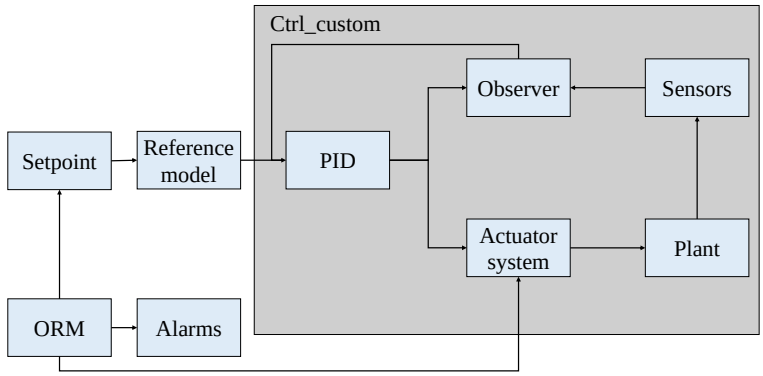

FIGURE 4.7: Representation of the ctrl_custom Simulink block diagram, along with elements added for the purpose of the thesis. ORM is short for Online Risk Model.

VeriStand is a software which can import control algorithms, simulation models and other tasks from a third-party environment. CyberShip Enterprise I is equipped with Veristand 2017 which is compatible with MATLAB 2016b. All MATLAB files and Simulink models are connected together in VeriStand.

The QTM software provides vessel data such as position and orientation of the model ship in the laboratory over Wi-Fi. Additional information is found in CyberShip I user manual (*CyberShip Enterpise I User Manual*).

4.3.4 GeNIE and jSMILE

GeNIe is used in order to create the BBN, which is a graphical user interface based on SMILE, Structural Modelling Inference and Learning Engine, which is developed in C++ and performs all calculations in GeNIe. The online risk model and control system developed in this thesis are programmed in Simulink and MATLAB. BayesFusion provides several fusions between SMILE and different programming languages. Consequently, a fusion written in Java called jSMILE is implemented, functioning as a bridge between MATLAB and SMILE. A tutorial on the implementation process is given on BayesFusion's website (Burkett, 2018). The connection between the hardware described above and SMILE was however unsuccessful, so experiments were done with pre-calculated values from the BBN.

Chapter 5

Conclusions and Further Work

This thesis has investigated the research area of autonomous ships, specifically on the topics of sea state estimation as a tool of gaining situation awareness, and risk-based decision making for an autonomous ship. This chapter makes some concluding remarks, and discusses further work on the topic.

5.1 Concluding Remarks

Situation awareness is a crucial aspect of an autonomous system. Without knowledge of the surroundings, the decision system will be unable to take the right actions. This thesis has investigated situation awareness in two quite differing ways, where the first was the development of a non-model based sea state estimation algorithm for a DP vessel, and the second was the construction of a decision model taking actions based on the collision risk level on an autonomous DP ship.

In *Paper A*, the first appended paper to this thesis, a sea state estimation algorithm capable of estimating the wave direction, significant wave height and peak wave period for a DP vessel was developed. The input to the estimation algorithm was preprocessed data for the vessel motion in all its DOFs, and what separates the method from previous methods is that it operates independently of the vessel transfer function which may be difficult to obtain. The wave direction was estimated using QDA, and was estimated with accuracy. The significant wave height and peak wave period were also estimated with promising results, comparable to model-based methods, using multivariate regression methods.

The second contribution of this thesis was a risk-based decision model for a DP autonomous vessel. The decision model made decisions based on the probability of collision, and the collision risk level was calculated using a BBN. The BBN was

constructed to account for a range of factors which can affect an autonomous vessel at a particular point in time, such as sensor failures, weather levels and power failure. Scenarios were constructed according to these factors, and the decision model was tested in model experiments in the MCLab. Results showed that the system was capable of making decisions based on the collision risk for the scenario in question.

In conclusion, although the two contributions differ in topics, they are both related to situation awareness and are highly relevant for autonomous ships research. A decision model for an autonomous ship is dependent on an accurate sea state estimation algorithm, as weather is a limiting factor in all marine operations.

5.2 Further Work

There are a number of ways in which further studies can be conducted on the topic of this thesis.

Firstly, a connection of the two specific contributions of this thesis could be done. An online on-board sea state estimation algorithm as input into a BBN, and further into a decision model could be of great interest. Testing this in full-scale experiments would constitute a wholistic system regarding weather situation awareness, as well as test the robustness of both of the contributions.

Additionally, an extension of both the sea state estimation algorithm and the decision model to apply for a vessel with forward speed is an interesting topic. Going towards autonomous shipping, situation awareness in transit is of utmost importance, related to weather, ships on collision course, and other objects nearby.

This leads to next topic of further work: object detection. In *Paper B* of the appended papers, perfect observation of the surroundings was assumed given that the relevant sensor was operative. Extending this to the use of proper sensors and an object detection system would make the work more realistic and would allow for highly advanced testing.

Lastly, further studies could extend the decision model to include projection of events, as done in Endsley's situation awareness model. The model as it is does project events as it anticipates a future collision, but this could be extended to other future events and account for the economic, environmental and human consequences related to future events and decisions being made.

References

Advanced Autonomous Waterborne Applications (AAWA) (2016). Remote and Autonomous Ships - The Next Steps. URL: https://www.rolls-royce.com/~/media/Files/R/Rolls-Royce/documents/customers/marine/ship-intel/aawa-whitepaper-210616.pdf (visited on 05/06/2019).

Akaike, H. (1980). Likelihood and the Bayes procedure. *Trabajos de Estadistica Y de Investigacion Operativa* 31.1, 143–166. ISSN: 0041-0241.

Andrade, F., Johansen, T. A., and Storvold, R. (2017). Autonomous UAV surveillance of a ship's path with MPC for Maritime Situational Awareness. URL: http://hdl.handle.net/11250/2471916.

Arneson, I. B., Brodtkorb, A. H., and Sørensen, A. J. (2019). Sea State Estimation Using Partial Least Squares Regression and Quadratic Discriminant Analysis. *Submitted to CAMS*.

Bole, A. G. (2005). *Radar and ARPA manual*. 2nd ed. Amsterdam: Elsevier Butterworth Heinemann. ISBN: 1-281-00946-6.

Brien, C. O. (2018). Key advantages and disadvantages of ship autonomy. URL: https://safety4sea.com/key-advantages-and-disadvantages-of-ship-autonomy/ (visited on 05/25/2019).

Brinchmann, P. A. Massterly: Autonomy in shipping; opportunities and challenges.

Burkett, J. P. (2018). A Bibliographic Guide to Methods for Causal Inference: Theory, Software, and Applications.

Clemente, S., Loia, V., and Veniero, M. (2014). Applying cognitive situation awareness to collision avoidance for harbour last-mile area safety. *Journal of Ambient Intelligence and Humanized Computing* 5.5, 741–745. ISSN: 1868-5137.

CyberShip Enterpise I User Manual. Faculty of Engineering Science and Technology, Department of Marine Technology, NTNU.

DNV GL (2007). DNV-RP-C205: Environmental Conditions and Environmental Loads.

DNV GL (2017). DNVGL-RP-N101 Risk management in marine and subsea operations.

DNV GL (n.d.). HIL Testing Concept Explanation. URL: https://www.dnvgl.com/services/hil-testing-concept-explanation--83385 (visited on 05/30/2019).

Endsley, M. (1995). Endsley, M.R.: Toward a Theory of Situation Awareness in Dynamic Systems. Human Factors Journal 37(1), 32-64. *Human Factors: The Journal of the Human Factors and Ergonomics Society* 37, 32–64. DOI: 10.1518/001872095779049543.

Endsley, M. (2000). Situation awareness analysis and measurement, chapter theoretical underpinnings of situation awareness. *A Critical Review*, 3–33.

Faltinsen, O. M. (1990). *Sea loads on ships and offshore structures*. Cambridge ocean technology series. Cambridge: Cambridge University Press. ISBN: 0521372852.

Fossen, T. I. (2011). *Handbook of Marine Craft Hydrodynamics and Motion Control*. Chichester, UK: John Wiley & Sons, Ltd. ISBN: 9781119991496.

Greco, M. (2012). TMR4215: Sea Loads - Lecture Notes. Department of Marine Technology, Faculty of Engineering Science and Technology, NTNU.

Huang, H. E. (2004). Autonomy Levels for Unmanned Systems Framework, Volume I: Terminology. *NIST Special Publication 1011*. DOI: https://doi.org/10.6028/NIST.sp.1011-I-2.0.

Huang, H.-M. (2007). Autonomy levels for unmanned systems (ALFUS) framework: safety and application issues. *Proceedings of the 2007 Workshop on performance metrics for intelligent systems*. PerMIS '07. ACM, 48–53. ISBN: 9781595938541.

IMO (2018). IMO takes first steps to address autonomous ships. URL: http://www.imo.org/en/MediaCentre/PressBriefings/Pages/08-MSC-99-MASS-scoping.aspx (visited on 05/28/2019).

Iseki, T. and Ohtsu, K. (2000). Bayesian estimation of directional wave spectra based on ship motions. *Control Engineering Practice* 8.2, 215–219. ISSN: 0967-0661.

Kapinski, J. et al. (2016). Simulation-Based Approaches for Verification of Embedded Control Systems: An Overview of Traditional and Advanced Modeling, Testing, and Verification Techniques. *IEEE Control Systems* 36.6, 45–64. ISSN: 1066-033X.

Kongsberg (2017). Yara and Kongsberg enter into partnership to build world's first autonomous and zero emissions ship. URL: https://www.kongsberg.com/maritime/about-us/news-and-media/news-archive/2017/yara-and-kongsberg-enter-into-partnership-to-build-worlds-first-autonomous-and/ (visited on 06/04/2019).

Kretschmann, L., ed. (2015). D9.2: Qualitative assessment, by the MUNIN project.

Liu, Z. et al. (2016). Unmanned surface vehicles: An overview of developments and challenges. *Annual Reviews In Control* 41, 71–93. ISSN: 1367-5788.

Lloyd's Register Group Ltd (2017). Global Marine Technology Trends 2030.

Lloyd's Register Group Ltd (2019). Autonomous Shipping 2019 and Beyond.

Marine Cybernetics Laboratory Handbook (2017). Faculty of Engineering Science and Technology, Department of Marine Technology, NTNU.

MUNIN (2016). Welcome to the MUNIN Project web page. URL: http://www.unmanned-ship.org/munin/ (visited on 06/02/2019).

Nielsen, U. and Iseki, T. (2012). A Study on Parametric Wave Estimation Based on Measured Ship Motions. *The Journal of Japan Institute of Navigation* 126. DOI: 10.9749/jin.126.171.

Nielsen, U. D. (2017). A concise account of techniques available for shipboard sea state estimation. *Ocean Engineering* 129, 352–362. ISSN: 0029-8018. DOI: http://dx.doi.org/10.1016/j.oceaneng.2016.11.035.

Nielsen, U. D. (2006). Estimations of on-site directional wave spectra from measured ship responses. *Marine Structures* 19.1, 33–69. ISSN: 0951-8339.

Norwegian Coastal Administration (2016). Automatic Identification System (AIS). URL: https://www.kystverket.no/en/EN_Maritime-Services/Reporting-and-Information-Services/Automatic-Identification-System-AIS/ (visited on 05/30/2019).

Pascoal, R. and Guedes Soares, C. (2008). Non-parametric wave spectral estimation using vessel motions. *Applied Ocean Research* 30.1, 46–53. ISSN: 0141-1187.

Pinkster, J. A. (1978). Wave Feed-Forward As A Means To Improve Dynamic Positioning. Offshore Technology Conference. *Offshore Technology Conference*. DOI: doi:10.4043/3057-MS.

Porathe, T., Prison, J., and Man, Y. (2014). Situation awareness in remote control centres for unmanned ships. ISBN: 9781909024243.

Prasad, D. K. et al. (2016). Challenges in video based object detection in maritime scenario using computer vision.

Rausand, M. (2011). Risk assessment : theory, methods, and applications. eng. Hoboken, N.J.

Rolls-Royce (2016). Rolls-Royce and Finferries demonstrate world's first Fully Autonomous Ferry. URL: https://www.rolls-royce.com/media/press-releases/2018/03-12-2018-rr-and-finferries-demonstrate-worlds-first-fully-autonomous-ferry.aspx (visited on 06/04/2019).

Rothman, P. (2018). RADAR vs. LIDAR: A Technology Toe-To-Toe. eng. *Security Dealer & Integrator* 40.10, 60–66. ISSN: 19410891. URL: http://search.proquest.com/docview/2123019745/.

Skredderberget, A. (2018). The first ever zero emission, autonomous ship. URL: https://www.yara.com/knowledge-grows/game-changer-for-the-environment/ (visited on 05/25/2019).

Sørensen, A. J. (2013). *Marine control systems: propulsion and motion control of ships and ocean structures, Lecture Notes*. Department of Marine Technology, Faculty of Engineering Science and Technology, NTNU.

Tannuri, E. A. et al. (2003). Estimating directional wave spectrum based on stationary ship motion measurements. *Applied Ocean Research* 25.5, 243–261. ISSN: 0141-1187.

Teknologien endrer samfunnet (2018). Bergen: Fagbokforlag. ISBN: 9788245023404.

Vartdal, B. J., Skjong, R., and St.Clair, A. L. DNV GL: Remote-controlled and autonomous ships.

Vinnem, J. and Utne, I. (2018). Risk from cyberattacks on autonomous ships. *Safety and Reliability - Safe Societies in a Changing World - Proceedings of the 28th International European Safety and Reliability Conference, ESREL 2018*. CRC Press/Balkema, 1485–1492. ISBN: 9780815386827.

Waals, O. J., Aalbers, A. B., and Pinkster, J. A (2002). Maximum likelihood method as a means to estimate the directional wave spectrum and the mean wave drift force on a dynamically positioned vessel. *21st International Conference on Offshore Mechanics and Arctic Engineering* 4, 605–613. DOI: doi:10.1115/OMAE2002-28560.

Øvergård, K. I. et al. (2015). Critical incidents during dynamic positioning: operators' situation awareness and decision-making in maritime operations. *Theoretical Issues in Ergonomics Science* 16.4, 366–387. ISSN: 1463-922X.

Paper A

Sea State Estimation Using Quadratic Discriminant Analysis and Partial Least Squares Regression

Ina Bjørkum Arneson, Astrid H. Brodtkorb, Asgeir J. Sørensen

Submitted to the Joint CAMS and WROCO 2019

Sea State Estimation Using Quadratic Discriminant Analysis and Partial Least Squares Regression

Ina Bjørkum Arneson * **Astrid H. Brodtkorb** *
Asgeir J. Sørensen *

* *Department of Marine Technology, Norwegian University of Science and Technology (NTNU), NO-7491 Trondheim, Norway (e-mail: inaba@stud.ntnu.no, astrid.h.brodtkorb@ntnu.no, asgeir.sorensen@ntnu.no)*

Abstract: This paper proposes non-model based sea state estimation methods for a dynamically positioned vessel. Sea state estimation entails finding the wave direction, significant wave height and peak wave period and is done based on sensor data of the vessel response. Sea state estimation is of importance because it assists the on board decision system and provides weather information for the relevant geographical position. In this paper, the methods for sea state estimation are based on machine learning algorithms, rather than the vessel transfer function. The models are trained and tested using simulated time series of response data, and yield promising results.

Keywords: Sea state estimation.

1. INTRODUCTION

Information about the sea state is necessary for decision making, securing safe marine operations. When using weather information from wave buoys, the weather for a specific position is found by interpolation between the positions of the wave buoys. On board sea state estimation may provide a more accurate sea state than information from wave buoys as it provides information in real time and for the specific position the vessel is in (Nielsen, 2017).

Nearly all marine operations have weather requirements. For example drilling operations, lifting operations and tandem operations all have strict limitations on significant wave heights. Input on real time sea state information for the exact geographical position allows for a better knowledge base for decision-making and potentially cost-savings related to waiting on weather or aborting an ongoing operation. As stated in Nielsen (2017), sea state estimation covers a wide range of purposes. Sea state estimation can be used for operational profiles, i.e. whether the ship operates in the conditions it was designed for, fuel performance evaluations, research on added resistance and accident investigations. The sea state is also of interest for autonomous ships, where the control system needs as much information as possible about the vessel surroundings and operational environment. Additionally, the sea state is an important input to the on board decision support system, as it for example can be used when detecting the occurrence of parametric roll (Galeazzi et al., 2015). Parametric roll is a phenomena which can cause serious damage, and the sea state may be a crucial input when deciding on measures to avoid parametric roll.

Previous work within the field involve model based calculation both in the time and frequency domain, for ships with forward speed and in Dynamic Positioning (DP). Most of the present day methods can be characterized as the so-called wave buoy analogy. The wave buoy analogy involves using a mathematical model to relate vessel response measurement data to the sea state. The common ground for many present model based methods is that they rely on some knowledge of the vessel's transfer function. The transfer function represents how waves are transferred into the vessel responses. Transfer functions are calculated using potential wave theory and sometimes Computational Fluid Dynamics (CFD) based on Navier-Stoke's equations and other nonlinear effects. Transfer functions can be difficult to estimate exactly, and if nonlinear effects are not accounted for, they will be inaccurate in severe waves.

Studies on sea state estimation for DP are extensive, and early studies include the use of the Maximum Likelihood Method by Waals et al. (2002). The method consists of calculating the Cross Power Spectral Densities (CPSD) using response data and minimizing the difference between this calculated spectrum and a theoretically found spectrum based on the phase difference and transfer functions. Further studies were done by Tannuri et al. (2003), who used a parametric estimation method. The directional spectrum was here represented by a 10-parameter function, capable of representing various sea states including doubly-peaked spectra. Similarly to Waals et al. (2002), the method further minimizes the difference between the measured and estimated response to yield the estimated sea state. Pascoal and Guedes Soares (2008) propose a non-parametric method which consists of an error minimization between CPSD based on sensor data and CPSD estimated using

the transfer function, where a smoothing term yielding a smooth spectrum is also included.

The main scientific contribution in this paper is the development of non-model based methods for sea state estimation using machine learning methods. A computationally efficient and accurate method for distinguishing between port and starboard waves, as well as head and following waves when relevant, is applied. The machine learning methods do not rely on transfer functions, and simply rely on estimating the sea state based on a combination of parameters calculated using the vessel response in all its Degrees of Freedom (DOFs).

The vessel used in the case study in this paper is NTNU's research vessel, R/V Gunnerus. A simulation model in Simulink was used to generate the data needed for the sea state estimation research.

This paper is organized as follows: Firstly in Section 2 the theory on wave modeling and vessel response is covered. Further, in Section 3 the theory behind the methods used for sea state estimation is described, followed by Section 4 including a description of how the sea state estimation algorithm combines these methods to produce results. Simulation results for estimation of wave direction, significant wave height and peak wave period are presented in Section 5. Lastly, the paper is concluded in Section 6.

2. THEORY

A description of the way waves are modeled in the simulations as well as the basis for the algorithm's ability to distinguish between port/starboard and head/following waves are covered in this section.

2.1 Modelling Waves

The standardized wave spectrum called the JONSWAP spectrum is used to model waves in the simulation model. The JONSWAP spectrum, or the Joint North Sea Wave Project spectrum, can be parametrized by the equation

$$S(\omega) = \alpha \frac{g^2}{\omega^5} \exp \frac{-5}{4} \left(\frac{\omega_p}{\omega} \right)^4 \gamma^{exp[-0.5(\frac{\omega-\omega_p}{\sigma\omega_p})^2]} \qquad (1)$$

where g is the gravitational constant, ω is the wave frequency, ω_p is the peak wave frequency, γ is a non-dimensional peak shape parameter, σ is the spectral width parameter and α is a parameter determining the shape of the spectrum in the high frequency range (Myrhaug, 2014). The JONSWAP spectrum can be directly related to significant wave height by

$$H_s = 4\sqrt{m_o} \qquad m_0 = \int_0^\infty S(\omega) d\omega \qquad (2)$$

where m_0 is the first spectral moment of the spectrum. The JONSWAP spectrum is a singly-peaked spectrum for fully developed sea, and simulations are done with long-crested waves.

Table 1 (Price and Bishop, 1974) shows realistic combinations of significant wave heights and peak wave periods. These sea states are used to generate a dataset with response data and the associated sea state.

Sea State	**Description**	$\mathbf{H_s}$ [m]	$\mathbf{T_p}$ [s]
0	Calm (glassy)	0	-
1	Calm (rippled)	0 - 0.1	4.87 - 5.66
2	Smooth (wavelets)	0.1 - 0.5	5.66 - 6.76
3	Slight	0.5 - 1.25	6.76 - 7.95
4	Moderate	1.25 - 2.5	7.95 - 9.24
5	Rough	2.5 - 4.0	9.24 - 10.47
6	Very rough	4.0 - 6.0	10.47 - 11.86
7	High	6.0 - 9.0	11.86 - 13.66
8	Very high	9.0 - 14.0	13.66 - 16.11
>8	Phenomenal	>14.0	>16.11

Table 1. Table of realistic combinations of significant wave heights and peak periods (Price and Bishop, 1974).

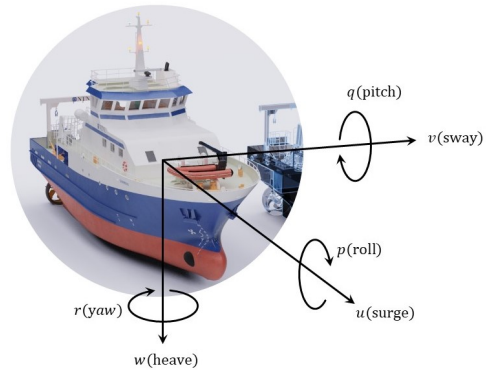

Fig. 1. R/V Gunnerus and its DOFs.

2.2 Differentiating Between Port and Starboard Waves

This section is based on information from Brodtkorb et al. (2018). Most vessels, including R/V Gunnerus, are port/starboard symmetric. This means that the response of the vessel is in practice the same for equal angles port and starboard of the center line. It therefore makes little sense to compare the energy in the sea state to distinguish between port and starboard waves.

In Figure 1 the DOFs in which the vessel can move, as well as the axes, are shown. The roll motions are anti-symmetric about the x-axis, meaning that when roll is negative on starboard side, it is positive on the port side and vice versa. On the contrary, the heave motions are symmetric about the x-axis. The cross-spectrum of roll and heave motions can therefore be used to estimate whether waves are incoming from port or starboard. In complex analysis, the imaginary part is an indication of the phase of the cross-spectra. It is therefore the imaginary part of the cross-spectra of heave and roll that can indicate if waves are incoming from port or starboard.

The following rule can be used to distinguish between port and starboard waves:

$$\hat{\beta} \in \begin{cases} [0°, 180°], & \text{if } \Gamma_{z\phi} \geq 0 \text{ (port)} \\ (-180°, 0°), & \text{if } \Gamma_{z\phi} < 0 \text{ (starboard)} \end{cases} \qquad (3)$$

where

$$\Gamma_{z\phi} = \int_{\omega=0}^{\omega_N} \text{Im}(R_{z\phi}(\omega)) d\omega \qquad (4)$$

and $\hat{\beta}$ is the wave direction estimate. $\mathrm{Im}(R_{z\phi}(\omega))$ is the imaginary part of the cross-spectra between the heave and roll motion and ω_N is the highest frequency.

2.3 Differentiating Between Head and Following Waves

This section is also based on information from Brodtkorb et al. (2018). Although R/V Gunnerus is not fore/aft symmetric, the response from head and following directions can be similar and difficult for the algorithm to distinguish. Correction of the initially estimated wave direction is therefore included. In a similar manner as for port/starboard waves, the imaginary part of cross-spectra can be used to distinguish between head and following sea. In this case, it is the heave and pitch cross spectrum that is relevant, as the pitch motion is anti-symmetric about the y-axis. Corrections for head and following wave directions are then made according to

$$\hat{\beta} \in \begin{cases} (0°, 90°), & \text{if } \Gamma_{z\theta} < 0 \text{ (following)} \\ [90°, 180°], & \text{if } \Gamma_{z\theta} > 0 \text{ (head)} \end{cases} \tag{5}$$

where

$$\Gamma_{z\theta} = \int_{\omega=0}^{\omega_N} \mathrm{Im}(R_{z\theta}(\omega))d\omega \tag{6}$$

$\mathrm{Im}(R_{z\theta}(\omega))$ is the imaginary part of the heave and pitch cross spectrum and ω_N is the highest frequency.

3. METHODOLOGY

This section includes a description of how the raw data is processed as well as theory on the methods used for sea state estimation. The methods include Quadratic Discriminant Analysis (QDA) used for estimating the wave direction, and Partial Least Squares Regression (PLSR) used for estimating the significant wave height and peak wave period.

3.1 Preprocessing of Raw Data

To obtain comparable values for the different sea states, the fast Fourier transform was used. The time series of the vessel response in all DOFs for each sea state were transformed to the frequency domain using the Fourier transformation. To obtain a single value for each DOF for the particular sea state, the frequency domain response was integrated over the frequency range. The results are then one response value for surge, sway, heave, roll, pitch and yaw for every sea state. These values, as well as the wave direction, significant wave height and peak wave period were then recorded and used as training data to make models to estimate the sea state.

3.2 Quadratic Discriminant Analysis

QDA is the method used for estimating the wave direction. Estimation of the wave direction is here considered a classification problem. Classification is a commonly used machine learning method, and involves classifying elements based on input data. The model is trained based on a training dataset with classes, which are the chosen wave directions. The output can therefore only be as precise as the training data. In practice this means that since the training data covers 18 different directions, the trained

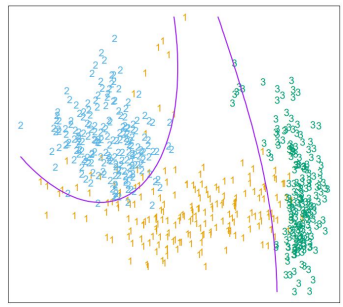

Fig. 2. Quadratic Discriminant Analysis (Hastie et al., 2001).

model can only output these 18 wave directions since these are the possible classes, i.e. the wave direction is discrete.

The remaining parts of this section are based on theory from Hastie et al. (2001). QDA models each class as a multivariate Gaussian function as follows:

$$f_K(x) = \frac{1}{(2\pi)^{p/2}|\mathbf{\Sigma}_k|^{1/2}} \exp -\frac{1}{2}(x-\mu_k)^\top \mathbf{\Sigma}_k^{-1}(x-\mu_k) \tag{7}$$

$\mathbf{\Sigma}_k$ is the covariance matrix for class k, μ_k is the mean for class k, and p is the number of dimensions. Unlike for Linear Discriminant Analysis (LDA), the covariance matrix, $\mathbf{\Sigma}$, is not the same for all classes. By working out the log ratio:

$$\log \frac{P(G=k|X=x)}{P(G=l|X=x)} \tag{8}$$

where l and k are classes, and using

$$P(G=k|X=x) = \frac{f_k(x)\pi_k}{\Sigma_{l=1}^K f_l(x)\pi_l} \tag{9}$$

one obtains a function where it can be seen that the decision boundary where $P(G=k|X=x) = P(G=l|X=x)$ is quadratic in x. K is the number of classes, and π_l is the prior probability of class l. The discriminant function for class k, δ_k, is shown in (10).

$$\delta_k(x) = -\frac{1}{2}\log|\mathbf{\Sigma}_k| - \frac{1}{2}(x-\mu_k)^\top \mathbf{\Sigma}_k^{-1}(x-\mu_k) + \log \pi_k \tag{10}$$

The boundaries between the classes are then defined by the function $\{x : \delta_k(x) = \delta_l(x)\}$. An example of boundaries on a plot of normally distributed mixtures is shown in Figure 2.

3.3 Partial Least Squares Regression

PLSR is a multivariate regression method which performs regression in one step by using the output data directly when decomposing the input data. PLSR aims to find new variables (latent variables) in the directions of both high variance and high correlation to the output (Hastie et al., 2001).

PLSR is based on the two equations below (Esbensen, 2001)

$$X = T \cdot P^\top + E \tag{11}$$

$$Y = U \cdot Q^\top + F \tag{12}$$

where X is the predictor variables, Y is the response variables and E and F are error terms. P and Q are latent

variables, meaning they are not the observed X and Y, but the new variables obtained through a mathematical model (Salkind, 2010).

Results shown in this paper are obtained using MATLAB which takes use of the SIMPLS algorithm. The first step in this algorithm is to centralize the data, i.e. give each column a mean of zero by subtracting the mean from every value. The SIMPLS algorithm uses Singular Value Decomposition (SVD), which finds the U, D and V satisfying the equation

$$X = U \cdot D \cdot V^\top \tag{13}$$

U and V are the left and right unitary matrices respectively, and D is a diagonal matrix of singular values. U and V are orthogonal matrices, where U contains the eigenvectors of the covariance matrix, $XX^\top$. V contains the eigenvectors of $X^\top X$ and D contains the non-negative square roots of the eigenvalues of $XX^\top$ (Golub, G. and Reinsch, C., 1970).

SVD is done on the matrix S, which is the product $X^\top Y$. The left singular vector from the SVD, U_a is multiplied by X to obtain t_a.

$$t_a = XU_a \tag{14}$$

This is an iterative process, so $a = 1, 2, ..., A$ where A is the number of latent variables, and hence also the number of iterations. t_a is then normalized by $t_{a,norm} = \frac{t_a}{\sqrt{t_a^\top t_a}}$, and used in the following calculations (Alin and Ali, 2012).

$$p_a = X^\top t_{a,norm} \tag{15}$$

$$q_a = \frac{D \cdot V}{t_{a,norm}} \tag{16}$$

Here p_a are the X-loadings, i.e. the coefficients transforming the X-variables to the new latent variables, and q_a are the Y-loadings, i.e. the coefficients needed to map the latent variables to the output, for iteration a. Both the X-loadings and Y-loadings are then orthonormalized through the modified Gram-Schmidt process. The iteration is then accounted for by deflating the S matrix as shown in (17).

$$S_{a+1} = S_a - v_a(v_a^\top S_a) \tag{17}$$

In the above equation the X-loadings have been orthonormalized and are denoted v_a.

When having obtained both X and Y-loadings, regression coefficients can be obtained which give a linear combination of the input variables mapping them to the output variables.

4. SEA STATE ESTIMATION ALGORITHM

The approach for estimating the sea state is based on a few steps. Firstly, the QDA model is trained to find the wave direction. The response of the vessel varies with varying wave directions, so PLSR is done for each of the wave directions. In practice, this means that each wave direction has an associated set of regression coefficients that can be used to estimate the significant wave height and peak wave period.

The wave direction is first found using the trained model. Based on the output from this model, the regression coefficients for the estimated wave direction are chosen and used to estimate the significant wave height and peak wave period. Figure 3 outlines the process.

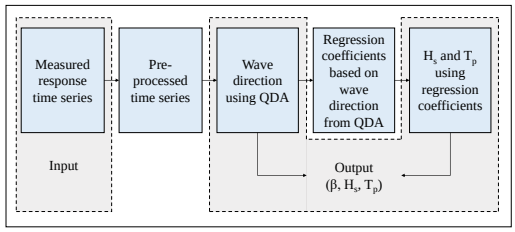

Fig. 3. Flow chart of sea state estimation algorithm.

Sea State	$\boldsymbol{\beta}$ [deg]	$\mathbf{H_s}$ [m]	$\mathbf{T_P}$ [s]
1	-163	2.0	8.3
2	161	2.7	9.4
3	-4	3.4	9.4
4	144	4.0	11.7
5	-140	4.7	11.3
6	-40	5.4	11.2
7	-35	6.1	12.1
8	-133	6.8	13.4
9	165	7.4	13.0
10	-159	8.1	12.5
11	-53	8.8	12.8
12	-175	9.5	14.6
13	-119	10.2	13.8
14	84	10.8	14.2
15	-18	11.5	14.0
16	-74	12.2	14.1
17	-112	12.9	14.2

Table 2. Sea states used to demonstrate sea state estimation results.

5. RESULTS AND DISCUSSION

This section presents sea state estimates using the methods described. The sea states in the results shown are made by deciding on a set of significant wave heights and randomly generating a peak wave period based on the ranges in Table 1, as well as a random wave direction. This means that the sea states will not be exactly the same as in the training data, which demonstrates the algorithm's performance on sea states other than the specific ones in the training data.

5.1 Simulation Results

The sea states used to demonstrate the algorithm's performance are shown in Table 2. Results for estimation of the wave direction are shown in Figures 4 and 5.

Results show that estimation of wave direction is done quite accurately. It is clear that for two of the sea states the algorithm unsuccessfully distinguishes between port and starboard waves. These sea states have incoming wave direction of $-163°$ and $-4°$, thus close to head and following sea respectively. The likely reason for the wrong estimation of the wave direction is that for these two sea states the roll motions are low and the heave-roll cross-spectra therefore carries limited information. Figure 5 shows the absolute value of the deviation in the wave direction.

As expected, nearly all sea states have an error of less than $10°$ as the classification algorithm is trained on data for

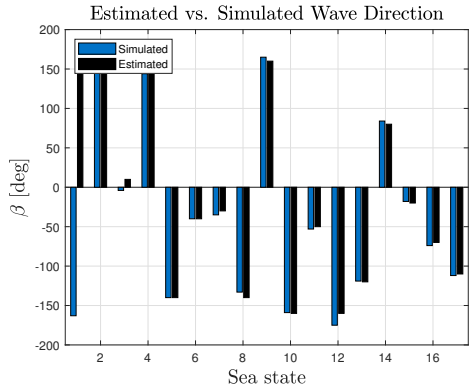

Fig. 4. Estimation of wave direction for sea states in Table 2.

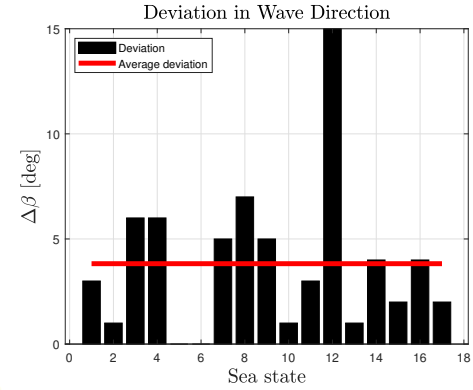

Fig. 5. Absolute deviation in wave direction for sea states in Table 2.

every 10th degree. The exception is sea state 12, which has a deviation of 15°.

Results showing the algorithm's performance on estimation of significant wave height are shown in Figures 6 and 7. Results show that the average deviation between simulated and estimated significant wave height is 0.7 m. Sea states 7-11 and 17 largely contribute to increasing this average with deviations up to 1.3 m. That deviations are large for higher sea states is expected as the method used is a linear method and in severe waves there are nonlinear phenomena present.

Figures 8 and 9 show results for peak wave period. The average deviation is 1.5 s, and many of the sea states are well below this average. However, especially sea state 16 largely increases the average deviation with a deviation of almost 4 seconds.

5.2 Discussion

Results demonstrated above are promising, and comparable to model-based methods. Comparing for example with results from Brodtkorb et al. (2018), the average deviation is approximately 0.25 m, which is significantly lower than average deviation presented above. However,

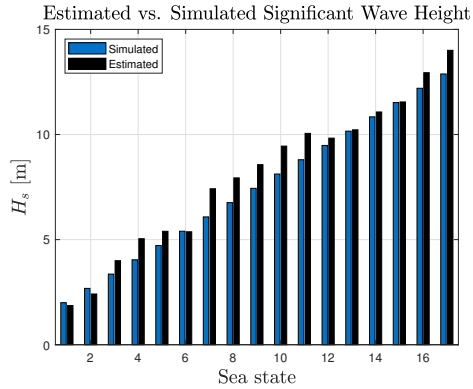

Fig. 6. Estimation of significant wave height for sea states in Table 2.

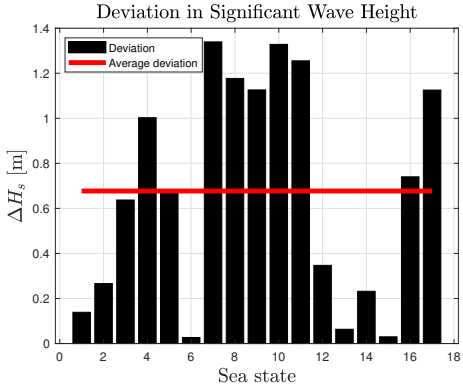

Fig. 7. Deviation in significant wave height for sea states in Table 2.

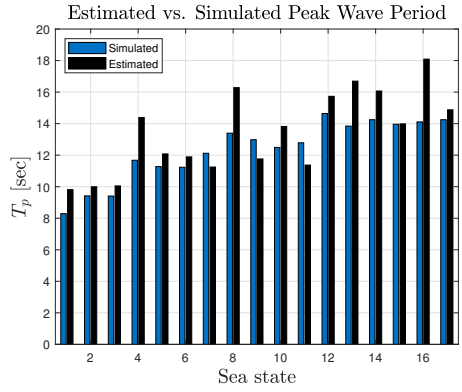

Fig. 8. Estimation of peak wave period for sea states in Table 2.

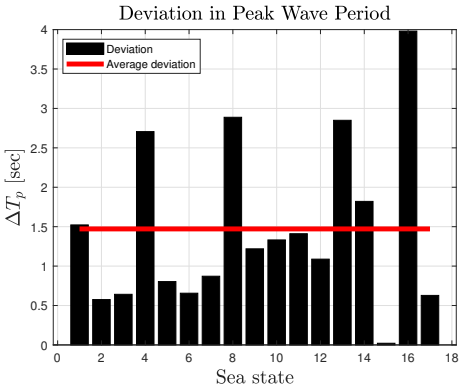

Fig. 9. Deviation in peak wave period for sea states in Table 2.

the results in Brodtkorb et al. (2018) are for a low sea state with $H_s = 2$m, where the algorithm in this paper also yields results of similar size. For the same sea state, the model-based algorithm gives a deviation in peak wave period of 0.1 rad/s, which is just above the average deviation presented in this paper of 0.06 rad/s. Nielsen (2007) demonstrates results for a vessel with forward speed, where the average deviation in significant wave height was 0.45 m using a parametric method. Average deviation in peak wave period was shown to be 0.96 s. This again was for low sea states with $H_s \leq 3$m. Although the algorithm presented in this paper performs at level with the model-based methods for many of the sea states, many of the estimated sea states yield much higher deviations, meaning that the robustness of the method can be questioned.

The strengths of the algorithm presented in this paper is that it requires little knowledge of the vessel, but rather relies on a large amount of collected data which can be obtained from sensors on the vessel. However, a weakness of the method is that it can be computationally inefficient to generate datasets carrying enough information to build a model. Additionally, the results presented are for perfectly long-crested waves. In practice this is seldom the case, so simulations for different types of sea states might be necessary for the method to be applicable at sea, as the response data generated for training would likely be different in short-crested, more realistic waves. Lastly, it may not be sufficient to use simulated data to develop models, as simulation models are unable to capture all phenomena and external effects present at sea.

6. CONCLUSIONS

The sea state estimation algorithm in this paper estimated wave direction, significant wave height and peak wave period with promising results. As expected, significant wave height and peak wave period have been estimated with more accuracy for lower sea states, due to nonlinear effects in more severe waves. The estimation algorithm for wave direction showed very accurate results, and a method for efficiently distinguishing between port and starboard waves has been presented.

Interesting continuance of the work presented includes testing the algorithms on full-scale experiments. This could yield a conclusion on whether simplified simulated data for training is in fact sufficient to develop algorithms applicable at sea.

Further, changing the spectrum used in simulations and thus allowing for higher variations in sea states would be interesting. Good results with a large variety of sea states would likely yield a model which is more applicable.

REFERENCES

Alin, A. and Ali, M. (2012). Improved straightforward implementation of a statistically inspired modification of the partial least squares algorithm. *Pakistan Journal of Statistics*, 28(2), 217–229.

Brodtkorb, A.H., Nielsen, U.D., and Sørensen, A.J. (2018). Online wave estimation using vessel motion measurements. *IFAC PapersOnLine*, 51(29), 244–249.

Esbensen, K.H. (2001). *Multivariate data analysis - in practice : an introduction to multivariate data analysis and experimental design*. Camo, Oslo, 5th ed. edition.

Galeazzi, R., Blanke, M., Falkenberg, T., Poulsen, N.K., Violaris, N., Storhaug, G., and Huss, M. (2015). Parametric roll resonance monitoring using signal-based detection. *Ocean Engineering*, 109(C), 355–371.

Golub, G. and Reinsch, C. (1970). Singular value decomposition and least squares solutions. *Numerische Mathematik*, 14(5), 403–420.

Hastie, T., Friedman, J., and Tibshirani, R. (2001). *The Elements of Statistical Learning: Data Mining, Inference, and Prediction*. Springer Series in Statistics,. Springer New York, New York.

Myrhaug, D. (2014). Marine dynamics: lecture notes 2009. Department of Marine Technology, NTNU, Trondheim.

Nielsen, U.D. (2017). A concise account of techniques available for shipboard sea state estimation. *Ocean Engineering*, 129, 352–362. doi: http://dx.doi.org/10.1016/j.oceaneng.2016.11.035.

Nielsen, U.D. (2007). Response-based estimation of sea state parameters influence of filtering. *Ocean Engineering*, 34(13), 1797–1810.

Pascoal, R. and Guedes Soares, C. (2008). Non-parametric wave spectral estimation using vessel motions. *Applied Ocean Research*, 30(1), 46–53.

Price, W.G. and Bishop, R.E.D. (1974). *Probabilistic Theory of Ship Dynamics*. Chapman and Hall, London.

Salkind, N.J. (2010). *Encyclopedia of Research Design*. SAGE Publications, Inc., Thousand Oaks.

Tannuri, E.A., Sparano, J.V., Simos, A.N., and Da Cruz, J.J. (2003). Estimating directional wave spectrum based on stationary ship motion measurements. *Applied Ocean Research*, 25(5), 243–261.

Waals, O.J., Aalbers, A.B., and Pinkster, J.A. (2002). Maximum likelihood method as a means to estimate the directional wave spectrum and the mean wave drift force on a dynamically positioned vessel. *21st International Conference on Offshore Mechanics and Arctic Engineering*, 4, 605–613. doi:doi:10.1115/OMAE2002-28560.

Paper B

Risk-Based Decision Making for Autonomous Ships: Collision Avoidance Case Studies

Ina Bjørkum Arneson, Emilie Thunes, Børge Rokseth, Ingrid B. Utne, Asgeir J. Sørensen

To be submitted to the IEEE Control Conference

Risk-Based Decision Making for Autonomous Ships: Collision Avoidance Case Studies

Ina Bjørkum Arneson * **Emilie Thunes** * **Børge Rokseth** *
Ingrid B. Utne * **Asgeir J. Sørensen** *

* *Centre of Autonomous Marine Operations and Systems, Department of Marine Technology, Norwegian University of Science and Technology (NTNU), NO-7491 Trondheim, Norway (e-mail: inaba@stud.ntnu.no, emiliet@stud.ntnu.no, borge.rokseth@ntnu.no, ingrid.b.utne@ntnu.no, asgeir.sorensen@ntnu.no)*

Abstract: This paper proposes an online decision model based on the risk of collision for an autonomous ship. A Bayesian Belief Network (BBN) has been constructed based on selected factors influencing the situation awareness and collision risk of the ship. Three scenarios have been defined, consisting of a sequence of events that increase the risk of collision. These are related to sensor failures, extreme weather and power shortage. A decision model has been made which makes decisions based on the collision risk and the events of the scenario in question. The method for risk assessment and decision making has been tested both in simulation and in model experiments.

Keywords: Risk analysis, autonomous ships, autonomous decision making, risk-based decision making, Bayesian Belief Networks, situation awareness

1. INTRODUCTION

Autonomous surface ships for transport of goods are expected to be in operation within the next years. For fully autonomous vessels to have maximum impact, they must be safer than humanly operated ships. For this to be possible, the vessel is dependent on extensive and accurate sensor data, and a decision system capable of processing this data and making intelligent decisions based on it. To name a few, location, surroundings and weather are factors necessary for the right decision to be made. The system must be able to identify and isolate failures, and handle deviations from normal operation (Utne et al., 2017). Risk should be part of the design process and operational phases of autonomous ships from the beginning to end, such that potential scenarios are identified and can be tested in simulation as early as possible.

Although highly autonomous ships are not operative in the nearest future, research on the risk related to autonomous ships is ongoing. Previous work within the field involve the MUNIN project, which presents the Maritime Intelligent Transport System (MITS) architecture (Rødseth and Tjora, 2014) which consists of scenario building, system modularization, hazard identification, risk control, hypothesis testing and design verification. The method firstly defines initial scenarios that could be relevant for an unmanned ship, and further divides the responsibilities related to the scenarios into different modules. Hazards are then identified and categorized, and then risk is assessed based on risk control options and cost benefits. Rokseth et al. (2019) propose a method for deriving a safety verification program for autonomous ships using Systems-Theoretic Process Analysis (STPA). The paper proposes a case study for a ship with autonomous navigation. The method is based on conducting STPA and developing a safety verification program which is a program consisting of simulations and tests to verify that certain hazardous events do not take place. The purpose of STPA is to identify hazards, Unsafe Control Actions (UCA) and their causes. Ramos et al. (2019) discuss the role of human operators in collision avoidance for autonomous ships. Hierarchial Task Analysis (HTA) is used to evaluate the performance of operators performing various tasks in a realistic environment.

For a traditional vessel, collision avoidance is usually based on human vision as well as Automatic Identification System (AIS) and Radio Detection and Ranging (RADAR) data to make decisions to avoid collisions. The Convention on the International Regulations for Preventing Collisions at Sea (COLREGS) are a set of rules for collision avoidance at sea, by the International Maritime Organization (IMO). COLREGS are also applicable for autonomous ships, imposing requirements on the sensor systems and the actions being taken in hazardous situations (Johansen et al., 2016). Johansen et al. (2016) propose a Collision Avoidance System (CAS) which searches for collision-free trajectories complying with COLREGS and which are close to the vessel's original trajectory.

According to Zhengjiang and Zhaolin (2003), common causes for collisions are

⋆ This work was supported by the Research Council of Norway through the Centres of Excellence funding scheme, project number 223254 NTNU AMOS.

Fig. 1. CyberShip Enterprise I. (Photo taken by authors of this paper.)

- Poor lookout
- Improper use of RADAR and Automatic Radar Plotting Aid (ARPA)
- Error of judgment
- Communication problems
- Failure to take early actions
- Apparently improper ship maneuvering
- Visibility

Many of the listed causes are a result of inexperience or poor training/skills. The factors listed above are all human effects and collision avoidance for a traditional vessels is done by avoiding these listed reasons. It is reasonable to assume that an autonomous system potentially may outperform humans in terms of some of these factors. For example, to avoid poor lookout and improper use of sensor data, sensor fusion is a possible method to give the vessel a realistic perception of the surroundings. Sensor fusion entails combining data from various sensors, such as RADAR, high definition visual cameras, thermal imaging and LIDAR into a realistic image of the surroundings (Advanced Autonomous Waterborne Applications (AAWA), 2016). Additionally, a control system that is able to make decisions based on the scenario in question may reduce the possibility of error in judgment, failure to take early actions and improper ship maneuvering.

Dynamic Positioning (DP) is an example of an autonomous operation where situation awareness (SA) is crucial. Developing complex and autonomous DP systems is an important stepping stone towards autonomous shipping (ABB, 2018). The applications for DP are typically to keep fixed position and heading of a vessel or rig, or to move from one place to another at low speed. Relevant operations include subsea installation and intervention, drilling and pipelaying (Sørensen, 2011). However, to develop a system which is autonomous from port to port, station-keeping and low-speed maneuvering capabilities are important for both docking and berthing. The scope of this paper is limited to a DP offshore vessel.

The vessel used in the case study and model experiments is CyberShip Enterprise I, pictured in Figure 1. CyberShip Enterprise I is equipped with one bow thruster and two Voith Schneider Propellers (VSP). As a DP case study is considered, diesel-electric propulsion is assumed, including redundancy in power generation in form of an extra generator capable of supplying full power.

The development and scientific contribution of this paper is a risk-based decision model for an autonomous DP vessel, including experimental results. Potential scenarios leading up to a collision may be complex and there may be a large number of potential scenarios. Furthermore, an infinite number of variations in how each scenario may play out, may be possible. Therefore, it is not feasible to predetermine and program the ship's response to any potential variation of each scenario. Furthermore, there may be uncertainty both in terms of observations (there may for example be uncertainty in terms of whether there is a ship nearby), and in terms of how observations ultimately will affect the collision risk. In the proposed method, it is assumed that the collision risk can be either "High" or "Low". Bayesian Belief Networks (BBNs) are used to calculate a "degree of belief" in the collision risk, which is represented by a probability distribution between the two states. Based on this probability distribution, as well as a belief regarding the events that are taking place, decisions regarding potential mitigating measures are made.

This paper is organized as follows: Firstly in Section 2, theory on BBNs and the specific BBN used to demonstrate results in this paper are covered. Further, in Section 3, the decision model is explained through a description of the algorithm and the case studies used in the experiments. Section 4 shows both simulation and experimental results. Finally, the paper is concluded in Section 5.

2. BAYESIAN BELIEF NETWORKS

This section starts by covering background theory on BBNs. This is followed by a description and explanation of the BBN used for simulations and experiments, which is used to calculate whether the risk of collision is sufficiently high to justify risk mitigating measures.

2.1 Preliminaries on Bayesian Belief Networks

A BBN is a graphical model that can be used to represent causality and uncertainty. In particular, BBNs are suitable for representing causal relationships between a set of variables and to assign a degree of belief that a variable is in a certain state based on incomplete knowledge about the state of other variables. In BBNs, degrees of belief are represented as probabilities (Darwiche, 2009). When BBNs are used for risk analysis, the objective is to estimate the degree of belief regarding whether or not accidents may occur and what consequences may follow. This can be done by identifying relevant factors that influence a critical event and illustrating the relationship between Risk Influencing Factors (RIFs). The probability of critical events can then be found, and the causes affecting the critical event the most can be identified.

The remaining part of this section is based on information from Rausand (2011). A BBN consists of nodes and directed arcs, where each node is a state or condition and arcs are directed towards the nodes that are influenced by this node. Figure 2 shows a simple BBN where the nodes

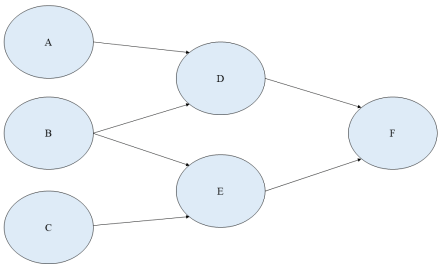

Fig. 2. Simple Bayesian Belief Network.

A, B, C, D and E represent RIFs that influence a critical event or hazard F.

In a BBN each node represents a variable that can have two or more possible states, or a continuous state. While the directed arcs indicate the structure of the causal dependencies between these variables, conditional probability tables quantify the relationships. The nodes on a direct path from A, are called the descendants of A, whereas a node that can be reached from A with one directed arc is its child. Similarly, the nodes that can reach A on a direct path are its ancestors, and the node that can reach node A with one arc is its parent.

Using Figure 2 as an example, some of the assumptions involved when using BBNs are demonstrated. If the state of node D is known, knowledge about the state in node A will not give additional information about state F. This means that when the state of a node is known, the node is independent of its ancestors. Looking at Figure 2, this can be described mathematically with the probability relationship

$$P(F|A \cap D) = P(F|D) \tag{1}$$

Additionally, a node is assumed to be conditionally independent in the network when states of all its parents are known. Using Figure 2, this can be described by

$$P(D \cap E|A \cap B \cap C) = P(D|A \cap B) \cdot P(E|B \cap C) \tag{2}$$

showing that nodes D and E are conditionally independent when the states of their parents are known. Lastly, it is assumed that two nodes are conditionally independent if there is no arc between them.

The software used for the construction of the BBN is called Genie, which is a graphical user interface for the SMILE engine. The SMILE engine is a learning/causal discovery engine, which specifically can be used for BBNs (BayesFusion, 2019).

2.2 The Bayesian Belief Network used in Simulations and Experiments

In this paper we assume that the collision risk-level can be either high or low, where a high collision risk level refers to a state in which the collision risk is unacceptably high. The BBN in Figure 3 can be used to calculate the degree of belief in the true state of the collision risk level (i.e. whether it is high or low).

The system SA depends on the communication between ship and the operator, the SA of the operator and the SA of the ship. As long as the vessel SA is maintained, the system SA is maintained, so the operator SA and communication with operator is only of relevance when the vessel SA is lost. If the vessel SA is lost and the operator SA is lost, the system SA is lost regardless of the communication. If the operator SA is not lost, but the communication fails, there is a high likelihood that the system SA is lost. In addition to communication from the ship, the operator can utilize drones to gain awareness of the surroundings. Wilhelmsen has already launched an autonomous drone to deliver parcels to ships (Wilhelmsen, 2019), so this technology could also be used to assist the operator to regain situation awareness for an autonomous vessel with sensor failures.

Under normal circumstances, the SA of both the ship and the operator depends on the navigation equipment (NE) aboard the ship. The purpose of the NE is to provide situation awareness of the surroundings. This equipment consists of a camera system, AIS, RADAR and a position reference system. Camera, AIS and RADAR all have the purpose of supplying information on what exists in the area around the vessel and on its collision course, and the position reference gives the vessel a position estimate. It is assumed that each of these systems can be either in a functioning state or in a failed state. The navigation system is assumed to have a high probability of functioning with only the RADAR working. However, with solely camera, AIS or position reference working, the probability of functioning NE is lowered, in the listed order. With only position reference functioning, the NE has a zero probability of functioning, as no data on the surrounding objects is available. Any combination of factors will obviously increase the probability of functioning NE compared to only one functioning sensor/equipment.

The weather and power aspects of the BBN are shown on the right side of Figure 3. The weather is represented by current, wind and waves, where the wave height is defined as the factor with most influence on the weather level. Loss of position refers to an event in which the vessel's DP system is not capable of keeping the ship at the desired position and/or heading. Extreme weather contributes to both loss of position and power loss. Loss of position can occur in the event of extreme weather, for example, if large waves or wind gusts temporarily force the vessel out of position, or if the maneuverability of the vessel is lost or reduced to an inadequate level. This may be caused by the loss of the vessel's thrusters, which in turn may occur due to inadequate power supply. Power loss can also be a result of unsatisfactory maintenance. Operating with only the bow thruster is considered a loss of maneuverability, and operating with one VSP yields some but poor maneuverability. It is also accounted for in this model that more severe weather conditions, increases the probability that the power supply and vessel maneuverability will be inadequate.

Lastly, the factor of having an object nearby is added as a node directly influencing the end event. Obviously, if there is nothing to collide with, there is no risk of collision.

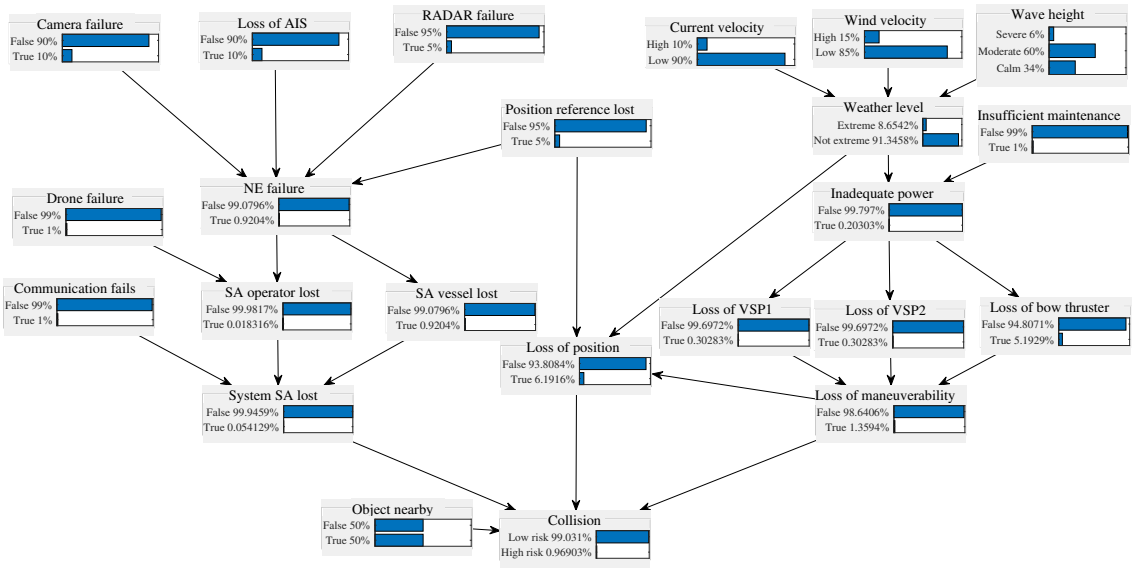

Fig. 3. BBN used in the risk-based decision model, with baseline evidence.

3. THE DECISION MODEL ALGORITHM

This section starts by explaining the flow diagram representing the algorithm used in the decision model. Further, the case studies are presented.

3.1 The Flow of the Decision Model Algorithm

Figure 4 shows a flow chart describing the process behind the decision model. The scenario can consist of defining the state of any of the nodes in Figure 3, i.e. the scenarios consist of a combination of states of the factors shown in Figure 3. The algorithm starts each time step by checking whether there has been a change in the scenario since the last time step. If the scenario has changed (i.e. some of the states or probability distributions in the BBN model have been altered), the collision risk-level probability distribution is updated using the relevant scenario and the SMILE engine. A decision to intervene with a mitigating measure, is taken in the event that the belief in a high risk level exceeds a threshold value. For demonstration purposes, this threshold is set to 6% for the collision risk level in the following case studies. Mitigating measures are chosen by checking if criteria for each mitigating measure are fulfilled, for example that the power needs to be inadequate in order to turn the extra generator on.

3.2 Case Studies

Although the BBN in Figure 3 does not address every factor that influences the collision risk, it is sufficient for demonstrating the method and functionality of the decision model. Possible scenarios include every possible combination of the factors in Figure 3. However, a few scenarios have been chosen and results will be shown for these scenarios:

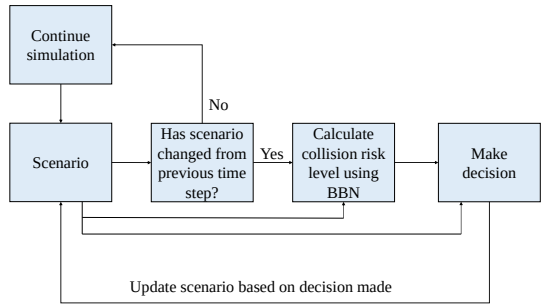

Fig. 4. Flow diagram of algorithm used for the risk model.

- Scenario 1: This scenario focuses on the effect of losing sensors. First of all, there is an object nearby. Further, camera, AIS and RADAR all fail consecutively. See the sequence of events in Table 1. The solution is that the vessel contacts the Shore Control Center (SCC), and the vessel is manually maneuvered away from the object it can collide with. The proposed mitigating measure for this scenario requires an operating drone with functioning communication to shore.
- Scenario 2: This scenario looks at the effect of weather and unsatisfactory maintenance. Again, there is an object nearby. The wave height is high, and the weather extreme. Later, evidence is received that maintenance has been unsatisfactory, all leading to higher risk of collision. The sequence is shown in Table 1. The mitigating measure here is to move the setpoint away from the object nearby.
- Scenario 3: In scenario 3 the vessel loses all its power. This causes the extra generator to be activated.

The scenarios are summarized in Table 1. The possible mitigating measures are thus defined as

- Change DP setpoint of vessel.
- Contact remote operator.
- Turn on an extra generator when no power is supplied to the thrusters.
- Turn on an alarm when evidence is received that maintenance has been unsatisfactory, operator is contacted, setpoint is changed, or extra generator is turned on.

The ship used in experiments is not equipped with sensors capable of object detection. As object detection is outside the scope of this article, it is simply assumed that the vessel is aware of its surroundings given that the relevant sensors are functioning. It is also assumed that the vessel is aware of the sea state, implying that an accurate on-board sea state estimation algorithm is available.

4. RESULTS AND DISCUSSION

This section presents the performance results of the decision model on the presented case studies, both in simulations and in the model experiments. Only scenario 2 is shown for simulations.

Simulations are done using a simulation model in Simulink, developed at NTNU. The model consists of a controller, observer, actuator system, vessel plant and sensor module. The controller takes the desired position as input, and this input changes according to the decisions being made by the risk-based decision system developed for this paper.

Model experiments are conducted in the Marine Cybernetic laboratory (MCLab) located at NTNU. The Qualisys Motion Capture System is used to track the vessel, using Oqus high speed infrared cameras. The VeriStand software is used to import the simulation model, making it compatible with various hardware necessary to control the vessel.

4.1 Simulation Results

Figures 5 and 6 show the simulation results for scenario 2. The sequence of events is as shown in Table 1, and the limit for the probability of high risk of collision is reached at the time when the state of "Insufficient maintenance" transitions from False to True. Due to these factors the setpoint is changed, such that the nearby object no longer is nearby and thus removing the risk of collision. Results show that CS Enterprise firstly makes its way towards the DP setpoint of [2 m, 0 m, 0°], and successfully makes the decision of changing setpoint to [6 m, 0 m, 0°] at 60 s. when the probability of a high collision risk-level exceeds the predefined threshold.

4.2 Experimental Results

Figure 7 shows the collision risk level for scenario 1, along with the predefined threshold of 6% and Figures 8 and 9 show the vessel position and path in model experiments. Scenario 1 entails alerting the SCC to manually maneuver the vessel away from the object nearby, given that the situation awareness of the vessel is lost and that evidence has not been received about the drone or communication with SCC failing. The system successfully alerts the SCC and the operator maneuvers the vessel away from its

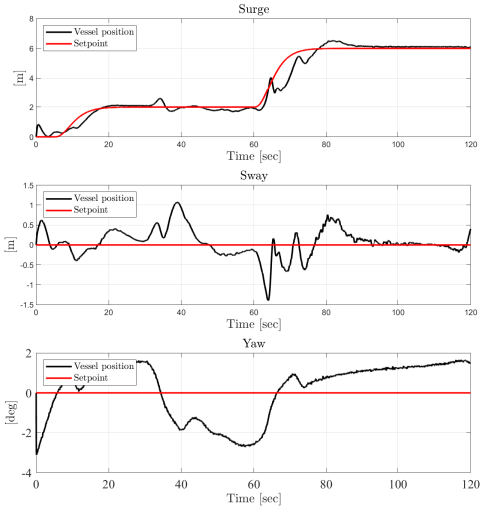

Fig. 5. Simulation results for scenario 2. Setpoint is changed at t = 50 s. Upper: surge position. Middle: sway position. Lower: yaw position.

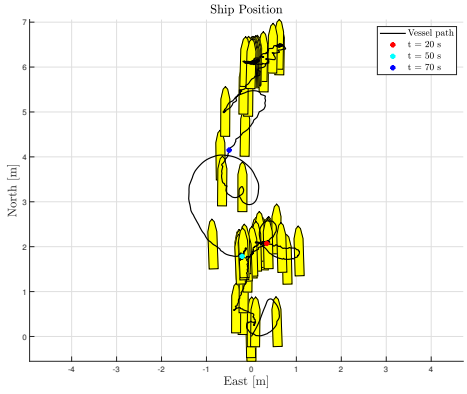

Fig. 6. Vessel path during scenario 2 in simulation. Setpoint is changed at t = 50 s.

position where the risk level for collision is above the selected threshold value. The risk level is reduced when the operator remotely takes control of the vessel. Figure 9 shows that when t= 50 s., the vessel moves in the direction of positive sway (manually), corresponding to Table 1 and Figure 7 where the threshold risk level is reached when the RADAR fails.

Scenario 2 was also tested in the model experiments, where the system received evidence of extreme weather

Table 1. Description of scenarios.

Scenario	Description	Event	Time of event [s]	Resulting probability of "high risk of collision" [%]
1	Focuses on the effect of losing sensors.	Object nearby = True	5 s.	1.9
		Camera fails = True	20 s.	2.1
		AIS fails = True	30 s.	2.2
		RADAR fails = True	50 s.	6.5
2	Focuses on extreme weather and unsatisfactory maintenance.	Object nearby = True	5 s.	1.9
		Wave height = Severe	20 s.	2.4
		Weather level = Extreme	25 s.	2.7
		Insufficient maintenance = True	60 s.	6.8
3	Focuses on power loss.	Object nearby = True	5 s.	1.9
		Inadequate power = True	30 s.	48.5

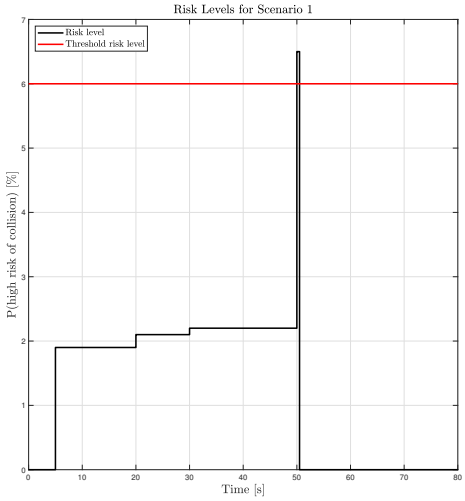

Fig. 7. Threshold risk value and collision risk level as a function of time for scenario 1.

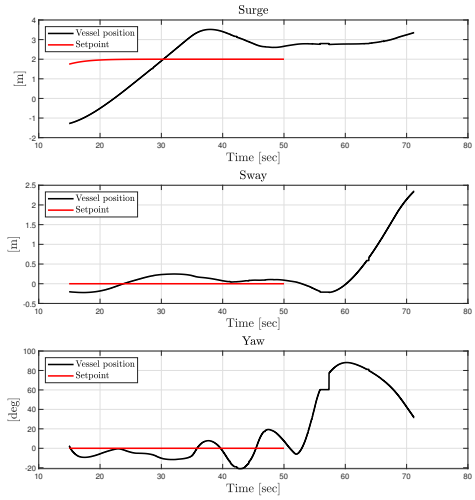

Fig. 8. Vessel position during scenario 1 in the model experiments. Vessel is manually maneuvered from t = 50 s.

and unsatisfactory maintenance, corresponding to the risk levels displayed in Figure 10. The reason for the small change in setpoint is to assure that the vessel stays within range of the cameras used for position reference in the laboratory. Figure 11 shows that the vessel changes setpoint at t = 60 s., although with an offset. The vessel did not have time to stabilize at its first setpoint before receiving a new setpoint at x = 3.5 m. Figure 12 shows that the vessel moves towards its first setpoint, overshoots and starts moving back towards the setpoint but is interrupted by the new setpoint and moves towards it. By the end of the experiment, the offset is still about 0.5 m., likely due to lack of time to stabilize.

In scenario 3 the power is turned off at 30 s., as can be seen by Figure 14 showing the control provided by thrusters. Figure 13 shows a largely increased risk level when power is lost. The power is out for 10 s. and the vessel struggles to keep its position during and after this time period, see Figure 15. Figure 16 shows that as expected, the vessel drifts when the power is lost, in the direction it was already moving. When power is regained, the vessel moves back towards the setpoint.

5. CONCLUSIONS

The decision model proposed in this paper demonstrated a method for assessing the risk of collision for an au-

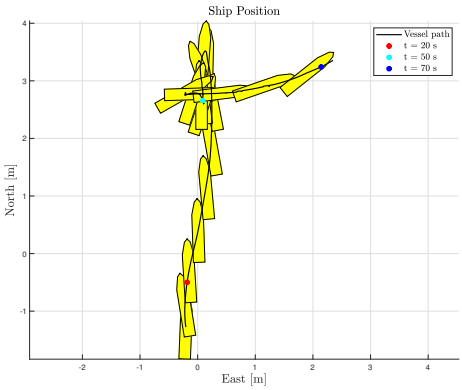

Fig. 9. Vessel path during scenario 1 for model experiments. Vessel is manually maneuvered from t = 50 s.

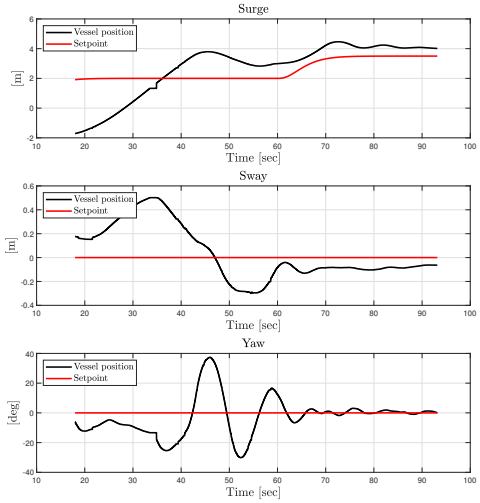

Fig. 11. Model experiment results for scenario 2. Setpoint is changed at t = 50 s. Upper: surge position. Middle: sway position. Lower: yaw position.

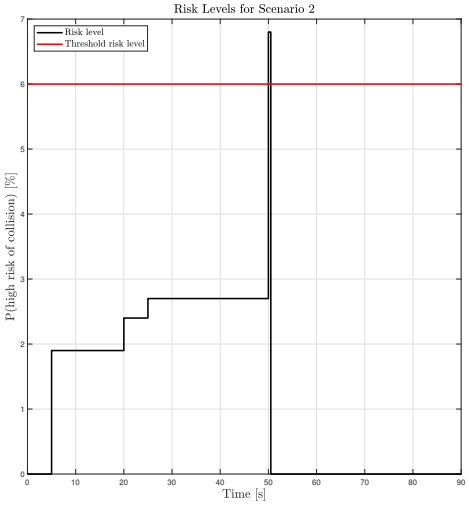

Fig. 10. Threshold risk value and risk level as a function of time for scenario 2.

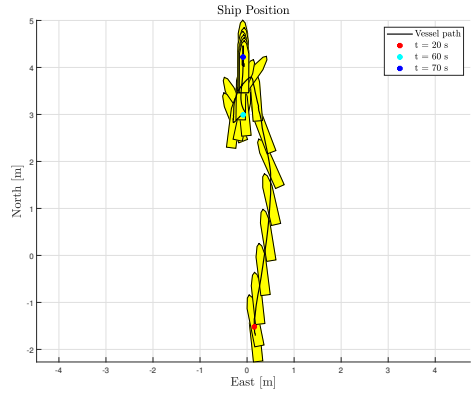

Fig. 12. Vessel path during scenario 2 in model experiments. Setpoint is changed at t = 50 s.

tonomous ship, and making decisions to remove this risk. The method has been experimentally tested and results showed that the vessel successfully made decisions and took action based on the events happening. Three scenarios have been tested, with three different outcomes.

Further work includes extending the BBN to contain more factors relevant for the risk of collision of an autonomous ship. Additionally, the possible mitigating measures have been limited to four different outcomes in this paper, so an extension of the possible actions should also be done. Extending the model to involve the projection of events would also greatly increase the applicability, as events can be foreseen and decisions can be made based on this. A threshold value for starting the extra generator should be included, as a high probability of inadequate power should trigger activation of the extra generator. This allows for indirect observations of the factor, and activation of the extra generator without direct evidence of "Inadequate

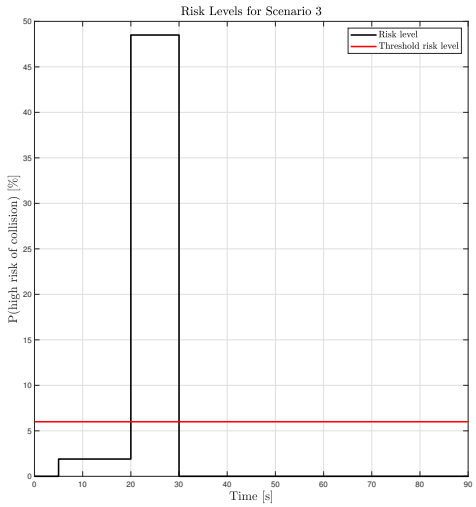

Fig. 13. Threshold risk value and risk level as a function of time for scenario 3.

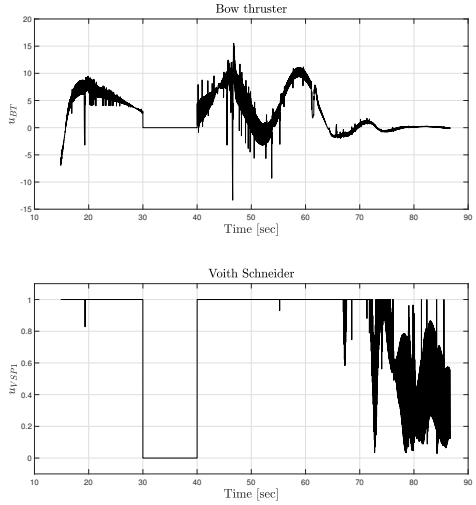

Fig. 14. Thrust in scenario 3. Upper is thrust for the bow thruster, lower is for one of the Voith Schneider propellers.

power". The BBN model should also be refined by considering more possible states for each variable. In general, variables with states that in reality are continuous, could be modeled with continuous probability distribution or a less coarse discretization. For example, the wind velocity, which in the model can take the values "High" or "Low", could be refined according to for example the Beaufort scale, or a continuous distribution. It is also assumed in the model that a sensor may either be working or failed.

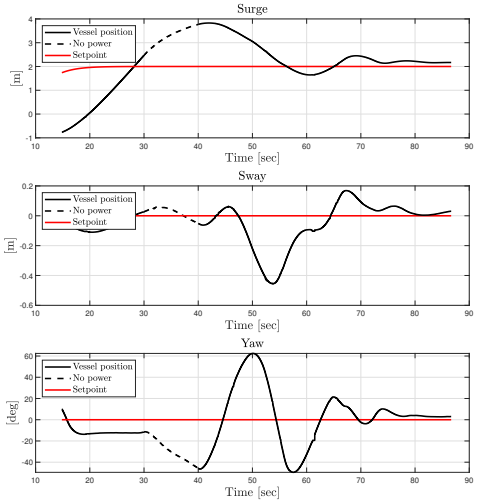

Fig. 15. Simulation results for scenario 2. Power is lost at t = 30 s. and regained at t = 40s. Upper: surge position. Middle: Sway position. Lower: yaw position.

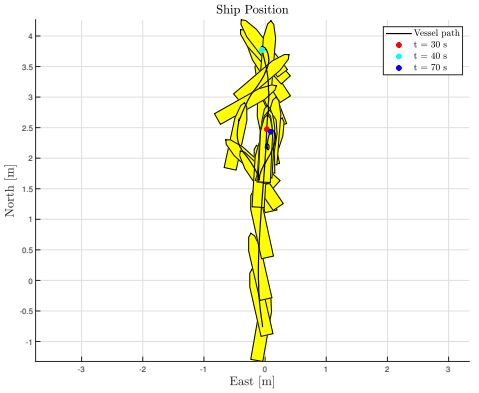

Fig. 16. Vessel path during scenario 3 in model experiments. Power is lost at t = 30 s. and regained at t = 40 s.

In addition to these states, other states, such as biased measurements, could be considered.

Combining the work presented with work related to object detection is also of great interest. The experiments here have been limited to assuming that the objects and events happening have been perfectly observed by the autonomous system. Testing on a vessel with sensors capable of object detection and sea-state estimation capabilities

would yield more realistic and applicable results, as there is uncertainty involved in trying to obtain SA. This also includes estimation of the sea state, as on-board sea state estimation algorithms also involve uncertainty.

REFERENCES

ABB (2018). Abb launches next-generation dp system, paving the way towards autonomous shipping. URL http://www.abb.com/cawp/seitp202/c473397fefeb1c08c12582fe0070673b.aspx.

Advanced Autonomous Waterborne Applications (AAWA) (2016). Remote and autonomous ships - the next steps. URL https://www.rolls-royce.com/~/media/Files/R/Rolls-Royce/documents/customers/marine/ship-intel/aawa-whitepaper-210616.pdf.

BayesFusion (2019). Smile: Structural modeling, inference, and learning engine. URL https://www.bayesfusion.com/smile/.

Darwiche, A. (2009). *Modeling and Reasoning with Bayesian Networks*, volume 9780521884389. Cambridge University Press, Cambridge.

Johansen, T.A., Perez, T., and Cristofaro, A. (2016). Ship collision avoidance and colregs compliance using simulation-based control behavior selection with predictive hazard assessment. *IEEE Transactions on Intelligent Transportation Systems*, 17(12), 3407–3422.

Ramos, M.A., Utne, I.B., and Mosleh, A. (2019). Collision avoidance on maritime autonomous surface ships: Operators tasks and human failure events. *Safety Science*, 116, 33–44.

Rausand, M. (2011). Risk assessment : theory, methods, and applications.

Rødseth, Ø. and Tjora, Å. (2014). A risk based approach to the design of unmanned ship control systems. *Maritime-Port Technology and Development*, 153–162.

Rokseth, B., Haugen, O.I., and Utne, I.B. (2019). Safety verification for autonomous ships. *MATEC Web of Conferences*, 273.

Sørensen, A.J. (2011). A survey of dynamic positioning control systems. *Annual Reviews in Control*, 35(1), 123–136.

Utne, I., Sørensen, A., and Schjølberg, I. (2017). Risk management of autonomous marine systems and operations. V03BT02A020. doi:10.1115/OMAE2017-61645.

Wilhelmsen (2019). Pilot launch in singapore: Autonomous drone delivery of parcels from shore to ship. URL https://www.wilhelmsen.com/ships-agency/maritime-drone-delivery/.

Zhengjiang, L. and Zhaolin, W. (2003). The human elements in ship collisions at sea. *Paper presented at the Asia Navigation Conference, 4th September 2003. Kobe, Japan.*